BRIGHT, LINFORD LAWRENCE. The Heat of Transfer of Some Slightly Soluble Salts from Water to tert-Butanol--Water Mixtures (1973). Directed by: John Robert Jezorek. Pp. 109

A group of slightly soluble salts have been investigated as probes in the study of water structure in organic--aqueous solvent systems. The probe reactions were run in pure water as well as tert-butanol--water mixtures at about 25°C. The enthalpies for AgI, AgTPB, and TPAsTPB precipitation were plotted versus mol % tert-butanol and these exhibited exothermic maxima at approximately 5.3 mol % tert-butanol. The maxima observed are discussed in terms of the contributions to the overall enthalpy change, and thought to be dependent on the structure of the solutions and the structure altering characteristics of the ions involved.

From the results of this investigation it was apparent that precipitation reactions can be useful in the study of water structure and water--solvent interaction. The precipitation reactions of AgTPB and TPAsTPB showed very large maxima of about 15 and 27 kcal respectively for the heats of transfer. Therefore AgTPB and TPAsTPB are shown to be excellent probes and should prove very useful in the investigation of other organic--aqueous binary systems. A further, tentative result is that TPB^- appears to be a structure making ion, from ΔS calculations in pure water.

THE HEAT OF TRANSFER OF SOME SLIGHTLY SOLUBLE SALTS FROM WATER TO TERT-BUTANOL--WATER MIXTURES

by

Linford Lawrence Bright III

A Thesis Submitted to
the Faculty of the Graduate School at
The University of North Carolina at Greensboro
in Partial Fulfillment
of the Requirements for the Degree
Master of Science

Greensboro
1973

Approved by

John R. Jezorek
Thesis Adviser

APPROVAL PAGE

This thesis has been approved by the following committee of the Faculty of the Graduate School at the University of North Carolina at Greensboro.

Thesis Adviser John R. Jezorek

Oral Examination Committee Members Harvey Herman

Walter V. Pattenbaugh

APR 1 3 1973

Date of Examination

ACKNOWLEDGMENTS

The author wishes to thank Dr. J. R. Jezorek for his guidance during this investigation and in the preparation of this thesis. To Margie Bright, the author wishes to express his gratitude and sincere thanks for her encouragement, motivation, and all her technical assistance in the writing of tnis thesis. The author would also like to express his appreciation to the staff of the Chemistry Department, of the University of North Carolina at Greensboro, for their encouragement and professional contributions. To Rebecca Barnard, the author expresses nis thanks for her time and skill in the typing of this thesis.

The author also wishes to acknowledge the assistantships from the University of North Carolina which provided financial support.

The author also wishes to acknowledge a grant from the Taylor George Steele Memorial Fund for the printing of this thesis.

L.L.B.

This thesis is dedicated in the memory of

Taylor George Steele

TABLE OF CONTENTS

LIST OF TABLES

LIST OF FIGURES

I. INTRODUCTION

Organic--aqueous solvent binary systems are of interest in solvent effect studies and water structure studies. An understanding of solvents will permit better analysis of the reactions occurring in this medium. Water structure has long been a topic of discussion, however its exact structure is still unknown.

Water is the most common and universally used solvent, but one of the least understood. Properties making water unique are its expansion upon freezing, high surface tension, liquid range, high boiling point, melting point, and critical temperatures relative to isoelectronic species. No theoretical calculations exist that give absolute information about a solvent as complex as water, or explain its unique characteristics. However, models have been developed to describe the structure of water and account for its unique properties. Much that is understood, and also many of the models have resulted from studies done on the solid water structure, the ice I structure. Work done by solid-state physicists has employed X-ray diffraction as the tool to study the ice I structure. The ice I structure has been used in these studies because structures and interactions in the solid state are generally more easily observed and described than those of the liquid state, since exact atom--atom distances can be obtained from the solid state, while only average atom--atom distances can be obtained from the liquid state. X-ray as well as Raman and infrared data have shown ice I to be a tetrahedral or distorted tetrahedral, three dimensional,

hydrogen-bonded structure. The hydrogen-bonded structures show intermolecular and intramolecular vibrations from the infrared and Raman spectra. Some type of distorted tetrahedron has also been indicated for the low temperature liquid model structure.

A useful technique in the study of water structure has been the use of organic--water solvent mixtures that show definite changes in a thermodynamic parameter for certain probes. Precipitation reactions, formation of slightly soluble salts, should be simple and straightforward to show these changes in thermodynamic parameters and their relationship to water structure.

It is hoped that a better understanding of thermodynamic parameters will increase the knowledge available concerning solvent effects and liquid water structure. At the present time, we must rely on hypothetical models which are generally special purpose models that must be tested against all data available to ascertain that the model is consistent with the data. As more and more data is accumulated, more characteristics of water will be revealed and new theories and models or adjusted models will be developed.

II. HISTORICAL BACKGROUND

A. Water Structure

The first suggestion that liquid water was structured came in 1884.[1] In 1891, Vernon postulated a structuredness of water to explain the phenomenon of maximum density.[2] Also in 1891, Röntgen qualitatively explained how ice melts at $0^{o}C$ and 1 atmosphere and the effect of pressure on its structural changes by using le Chatelier's Principle. Röntgen also postulated water as having polystructures, and while he did not propose any specific model, his theory is the seed of the so-called mixture models.[3] In 1900, Sutherland also represented water as a mixture of monohydral (steamlike), dihydral (dimeric, liquid), and trihydral (trimetric, icelike) species, but no experimental data was generated to verify his theory at that time.[4]

In 1933 Bernal and Fowler postulated the first plausible model for liquid water. This model, a forerunner of what is now called the uniformist model, assumed water to have an electrostatic character and exhibit simple coulombic interactions between rigid point charges. Thus, the electrostatic bond could bend but could not break. This model was based on the data collected to describe the ice I structure which predicted by X-ray analysis that hydrogen bonds would bend but not break.[5] The Bernal and Fowler model was followed by the Frank's and Evans' "iceberg" concept (1945), a mixture or two state model later called the flickering cluster model, which was formulated to explain data concerning the solvating of solute particles.[6]

About the same time, Samoilov attempted to account for the density of water by postulating that individual molecules could be shaken loose from the lattice which would then rearrange itself, enclosing these molecules in the lattice cavities. Samoilov's description was the prototype for the interstitial model. Because it described only a short range interaction, the model showed two distinct variations, and like the flickering cluster model, it was described as a mixture or two state model.[7] Danford and Levy, independent of Samoilov, also postulated an interstitial model in 1962, simulating the model from X-ray data. The model consisted of layers of puckered six-membered rings having interstitial water molecules to account for the change in density.[8] Pauling suggested a clathrate model (pentagonal dodecahedron) similar to a chlorine hydratelike structure. To explain density changes, Pauling believed one or more unbonded water molecules were guest components in the clathrate structure. His model was regarded as a water hydrate.[9]

Lennard, Jones, and Pople have used a statistical-mechanical approach to project a uniform model, the L. J. P. model, which invokes bond bending to explain physical and chemical changes in water structure. The L. J. P. model, after its introduction in 1951, was accepted more readily than previous models because chemists and physicists believed all molecules were under identical influences and environment, and thus should interact and appear similar in respect to one another. Also, all spectral data generated revealed only one peak, indicating the existence of a single type of vibrational mode which signified a uniform structure for water.[10] However, because difficulties arose when applying

the L. J. P. model to solutions and some thermodynamic data, Frank and Wen have proposed the use of the flickering cluster model to explain experimental results when the L. J. P. model failed.

Frank's and Wen's model (1957) was described as a flickering cluster model consisting of hydrogen-bonded and nonhydrogen-bonded structures.[11] Hoggis, Hasted, and Buckanan have observed molar lengthening of the relaxation wavelength which supported the flickering cluster model.[12] Thus, experimental results such as entropy, heat capacity, temperature of maximum density, tracer self-diffusion, thermal conductivity, dielectric relaxation, viscosity, and ionic mobility which were not explained by a uniform water structure were accounted for by the flickering cluster model.[11]

Probably the most important water model to date is that of Walrafen, based on infrared and Raman scattering spectroscopic analysis data. He has postulated a mixture model or a two state interstitial model based on the existence of 0, 1, 2, 3, and 4 hydrogen-bonded molecules and which relies on the interstitial model to explain changes in density and other physical and chemical properties of water. This model, a special purpose model, was based on data which seem reliable.[13]

With new and improved methods of analysis, such as X-ray diffraction and Raman spectroscopy, Walrafen and other workers have been able to obtain data which can be related more directly to liquid water structure. The data has led to new formulations and predictions resulting in a more creditable liquid water model.

The first stepping stone to a modern plausible model of water structure was the elucidation of the ice I structure, indicating the existence of four hydrogen-bonded molecules, revealing a tetrahedral structure. Studies have shown the tetrahedral ice structure to be distorted to some degree by pressure, but no hydrogen bond breaking was observed or postulated during the ice structure investigations.[14]

However, theoretical calculations have been made to predict various properties of hydrogen bonding in water by Rao and coworkers. Rao has used ab initio (nonempirical self-consistent field) calculations of the form CNDO/2 (complete neglect of differential overlap) in calculating the dissocation energy, D_e, of hydrogen bonds. First he considered the energy of hydrogen bonding in water, assuming its structure to be dimeric, and subjected the ab initio calculations to three possible dimer structures given below:[15,16]

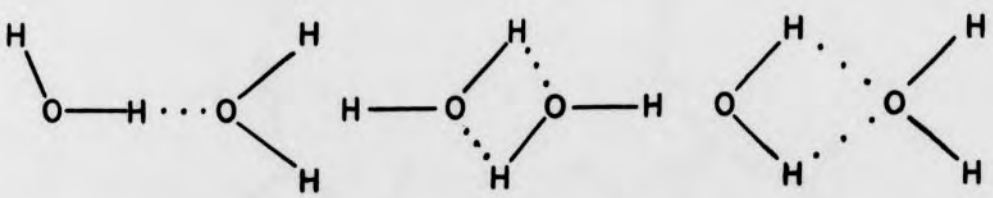

Linear (a) Cyclic (b) Bifurcated (c)

Calculation results indicate that the linear dimer is the most stable of the three models. Further calculations show that D_e values change very little when θ, the angle of deviation from two linearly-bonded structures, ranged from 0^o to 20^o, but when the angle increased above 20^o, the D_e values decrease significantly. Thus, the most stable linear dimer situation exists when θ measures between 0 and 20^o. Rao also has made calculations on five other structures -- 3 open trimers, 1 tetramer, and 1 pentamer.[17]

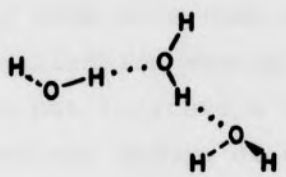

(d)

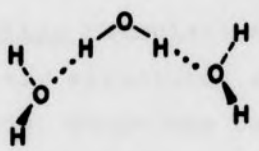

(e)

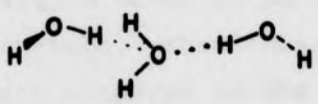

(f)

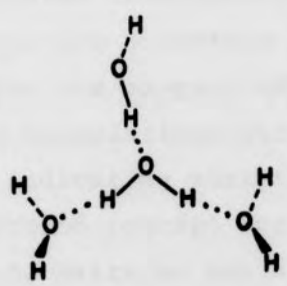

(g)

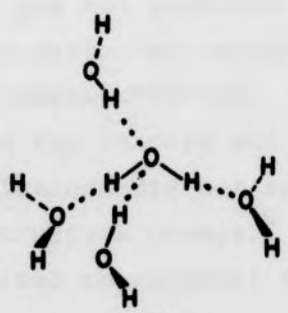

(h)

The largest D_e was determined for structure (e), indicating that it was the most stable.[17] However, Hoyland and Kier have found structure (f) to be the most stable configuration.[18] In addition, the tetramenter and pentamer did not appear more stable than the most stable trimer. DelBene and Pople have postulated that cyclic polymers may exist and ab initio calculations show the cyclic systems are more stable than the linear structures. Also, asymmetric cyclic structures are found to be more stable than symmetric cyclic structures.[19] This points out that water could possibly have more than one structure and still not lose its stabilization energy. These ab initio calculations, which do not indicate a tetrahedral water structure, support the model and theory of Danford and Levy, which has been previously introduced as a six-membered ring, having interstitial unbonded water molecules. They have found oxygen--oxygen distances in liquid water to be 1.10 Å, 2.88 Å, and 4.90 Å by X-ray diffraction. When these oxygen--oxygen distances of water were compared to the average of 5.5 Å for oxygen--oxygen distances in the ice I structure, the difference indicated intuitively that it was not possible for the tetrahedral ice structure to become distorted enough to account for the oxygen--oxygen distances observed. Thus, the ab initio calculations strengthened the Danford and Levy model by indicating that the calculations did not support the distortion concept for water structure change.[8] On the other hand, Walrafen has also utilized tetrahedral four-bonded configurations in formulating his model. As has been previously stated, he used infrared and intermolecular and intramolecular Raman spectral analysis to obtain reliable

data upon which he based his water model. Intramolecular Raman studies indicate that tetrahedral hydrogen-bonded and nonbonded structures exist simultaneously over a temperature range of supercooled to supercritical water. The data show that no hydrogen-bonded structures of 3, 2, or 1 have been isolated.[13,20,24] Walrafen has also subjected H_2O and D_2O to Raman scattering. The results reveal a broad but weak band centered at 60 cm^{-1}. Infrared absorption coefficients and neutron inelastic scattering also show bands at about 60 cm^{-1} which decrease with increasing temperature. Neither of the three bands are intense enough to be used alone as evidence of Walrafen's model. However, since all of the bands occur on their respective spectra and decrease with increasing temperature, the data strengthens the hydrogen bond breaking concept, therefore Walrafen's model.[25] In addition, infrared absorption in I ice has been reported at 65 cm^{-1}, which strengthens the analog computer indications of the weak infrared peak at 60 cm^{-1} for liquid water.[26] This band had previously been predicted in theoretical calculations by postulating a fully hydrogen-bonded, five-molecule tetrahedral structure with approximately C_{2v} point group symmetry.[13,21,25,27] Raman spectra also show an intense band at about 170 cm^{-1}.[25] The 170 cm^{-1} absorption band has also been observed by infrared studies and neutron inelastic scattering spectra from liquid H_2O and D_2O.[28] This band has been attributed to O-H...O or O-D...O stretching frequencies, respectively. As the temperature was increased from -60°C to 94.7°C, the intensities of the two bands decreased.[25] This observation has been verified by Blatz and interpreted as O-H...O or O-D...O structural breakdown.[29]

Librational or restricted rotational components of H_2O and D_2O appear in Raman, hyper-Raman, and neutron inelastic scattering spectra as broad contours which are an indication of overlap. Librational Raman bands of liquid H_2O occur in the range 200-1100 cm^{-1} and of liquid D_2O in the range of 150-300 cm^{-1} which overlap the Raman hydrogen stretching and librational contours. When water was studied over a temperature range of 10°C to 90°C, the librational Raman contour intensity decreased with an increase in temperature. The librational Raman contours have been subjected to decomposition by the analog computer technique into Gaussian components. The Gaussian components are centered at 425, 550, and 740 cm^{-1}. The temperature effect indicates a structural breakdown and the analysis of three components present indicate that the differences are in the degree of structure present.

All the data obtained from Raman scattering and infrared absorption plus the data from inelastic harmonic light scattering (Hyper-Raman), neutron inelastic scattering, and stimulated scattering at low temperatures can be shown to be consistent with the requirements of the C_{2v} point group. With assignments being made to a fully hydrogen-bonded C_{2v} structural model, interpretation at higher temperatures is easier. This consistency of data at low temperatures implying a C_{2v} symmetry was expected.[13] X-ray data by Morgan and Warren have shown low temperature liquid water tends toward a tetrahedral structure and that ice I definitely shows this tetrahedral structure.[30]

Probably the most important and latest significant addition to the development of a water model has come about

as additional Raman studies have been made, once again by Walrafen on H_2O and D_2O mixtures. Dilute solutions and 50% solutions of H_2O in D_2O solvent and D_2O in H_2O solvent were subjected to Raman spectroscopic studies. In the intramolecular valence region, 2000-4000 cm^{-1}, principle contributions come from OH and OD stretching vibrations of HDO, the major component of a 50% H_2O-D_2O solution. Components were H_2O, D_2O, and HDO existing in an approximate ratio of 1:1:2, respectively. Two maxima are observed in the Raman spectrum. One maximum appears at 3415 ± 5 cm^{-1} which has been assigned to OH stretching frequencies of HDO and H_2O. A second maximum appears at 2495 ± 5 cm^{-1} which refers to OD stretching frequencies of HDO and D_2O. Visible shoulders appear on both principal broad band peaks. One shoulder appears at 3625 ± 10 cm^{-1} and another appears at 2650 ± 10 cm^{-1}, referring to OH and OD stretching vibrations. Upon further scrutiny a third shoulder has been found at 3300 cm^{-1} and a fourth at 2400 cm^{-1}, assigned also to OH and OD stretching vibrations. The two more prominent shoulders at 3625 and 2650 cm^{-1} are believed to result from the nonhydrogen-bonded OH and OD stretching vibrations. The weaker shoulders are believed to result from coupling interactions between HDO molecules plus coupling components of H_2O and D_2O which appear at about 3250 cm^{-1} and 2370 cm^{-1}. Intermolecular coupling has been reduced tremendously by preparing a 1 mole percent H_2O and D_2O solution and lowering the HDO concentration. The intramolecular coupling was not reduced. The Raman spectrum of 1 mole percent solutions indicates appropriate maxima at 3435 cm^{-1} and 2530 cm^{-1}, and shoulders appear at 3626 cm^{-1} and 2650 cm^{-1}. The bands at 3435 cm^{-1}

and 2530 cm^{-1} refer to the hydrogen-bonded OH and OD stretching vibration frequencies, respectively. The shoulders at 3628 cm^{-1} and 2650 cm^{-1} refer to the nonhydrogen-bonded OH and OD stretching vibration frequencies, respectively, from the same solution. These data exhibit the first reliable evidence of the existence of nonhydrogen-bonded structures in liquid water. Raman spectra from 11 mole percent D_2O in H_2O obtained in the temperature range from 32.2°C to 93.0°C exhibit an isosbestic frequency, indicating that an equilibrium exists between the nonhydrogen-bonded and hydrogen-bonded OD stretching components, and that the band shapes, positions, and half-widths are approximately invariant in that temperature range. The frequencies are half-widths of the four Gaussian infrared absorption frequencies and are in reasonable agreement with the four Gaussian quantities from the argon-ion-laser Raman spectra reported above. These four vibrational frequencies are not as apparent in the infrared spectra as in the Raman, but this evidence considered together with the other spectral data discussed above, had a major effect on the formulation of a modern water structure model.[13,20,24]

X-ray diffraction data, as well as Raman and infrared data has made contributions in the development of models for liquid water. The most extensive study of water by X-ray diffraction has been at Oak Ridge National Laboratory by R. W. Hendricks, interpreted by Narten and Levy. This work was started in 1961 and is still in progress today. Narton and Levy have interpreted from small angle scattering that the position correlation of molecules is short range, which means that the density fluctuations are only of the

degree expected for a single phase or single chemical species. The absence of large density fluctuations has ruled out mixture models, such as the flickering cluster model, where large density fluctuations are inherent in the model.[7,31] In addition, a 10% increase in bulk density has been observed when going from 0° to 4°C, which is in agreement with a 10% increase in the coordination number from 4, for the tetrahedral structure, to 4.4 for the interstitial model.[1] The 4.4 coordination number had been derived from the X-ray peak around 2.9 Å, assigned to near-neighbor interactions at all temperatures between 4° and 200°C.[32] In addition, the increase in the near-neighbor distances from 2.84 Å at 4°C to 2.94 Å at 200°C indicates a weakening of O....H-O hydrogen bond at high temperatures.[33] Thus, these facts from X-ray analysis also favor an interstitial type model.

The data and conclusions presented appear to have made the mixture or two state model, mainly the interstitial model, the most reasonable choice, and has decreased the credibility of the uniformist model. The interstitial type, mixture model, is still subject to changes and greater characterization, but the basic pattern now seems to be set.

B. Alcohol Solvent Structures

By slightly perturbing a system to be studied, its peculiarities are magnified. Following this premise, the structure of water has been studied by adding varying amounts of alcohol to the system. Franks and Ives have studied alcohol--water solvent systems, primarily ethanol--water mixtures.[34] Arnett and coworkers have made extensive

investigations of tert-butanol--water solvent mixtures. From their results, these workers concluded that the structure of alcohols should be studied to determine their influence on the structure of water.[35]

Unlike water, which has a three-dimensional structure, alcohols have a two-dimensional structure. When the two structures are compared, water is a more structured, therefore a more complex entity. Even though both alcohols and water exhibit hydrogen bonding, alcohols lack many of the peculiarities which characterize water.[34]

The model for alcohols was formulated as a result of X-ray analysis and dielectric relaxation time studies. In 1935, Zachariasin concluded from X-ray radial distribution curves that alcohols were linear polymers of varying lengths existing in equilibrium with each other.[36,38] Liquid alcohols show a range of dielectric relaxation times, typically 10^{-9}, 10^{-10}, and 10^{-11} seconds. The residual high frequency margin between the dielectric constant and the square of the optical refractive index are attributed to librational and atomic polarizations. The relaxation times are studied within a homologous series by subjecting the alcohol to freezing and variation of temperature which indicated polymer chain destruction into doubly hydrogen-bonded, singly-bonded, and free molecules. Thus alcohols are described as existing in rapid equilibrium of very short-lived polymeric chains having assorted definite lengths and possessing a degree of rigidity because of considerable hinderance to internal rotation.[39]

Substantial evidence showing that high polymer chain lengths are favored has been revealed from standard

enthalpies and kinetic studies. Standard enthalpy changes signify that the stability of tetramers is enhanced as compared to dimers for methanol and sec-butanol whose standard enthalpy values are known. The general reactions are:

$$2\ ROH \longrightarrow (ROH)_2 + \Delta H_2^{\circ} \qquad \text{Eq. 1}$$

$$4\ ROH \longrightarrow (ROH)_4 + \Delta H_4^{\circ} \qquad \text{Eq. 2}$$

For methanol, the enthalpy values are 4.470 kcal/mole and -30.060 kcal/mole.[40] For sec-butanol, the enthalpy values are -5.250 kcal/mole and -23.118 kcal/mole.[41] The increase in enthalpy indicates greater stability for the longer polymer chain.

Equilibrium constants have been determined from NMR studies. These studies show the first association step $K_{1,2}$ was different from subsequent association steps, $K_{N,\ N+1}$. A single value exists for all equilibrium constants involving a reactant structure having five or more molecules per structure. Equilibrium constants K_{12} and K_{23} for tert-butanol were determined to be 6.75 and 111 $mole^{-1}$, respectively. These values indicate an increase in reactivity and polarity for the shorter chains, thereby indicating greater stability for the higher polymeric chains.[40]

Based on latent heats of fusion and latent heats of vaporization, Reid, Connor, and others believe that alcohols exist as cyclic polymers. Alcohols exhibit the normal latent heats of fusion and melting points implying little hydrogen bond breaking in this phase change. However, alcohols also exhibit abnormal latent heat of vaporization and boiling points implying much hydrogen bond breaking.[9,43] According to the cyclic model, alcohols, upon melting, go from the solid state to a cyclic liquid state which requires

little hydrogen bond breaking and therefore yield a normal latent heat of fusion. However, upon vaporization, the cyclic structures themselves must be broken, a process which involves significant amounts of hydrogen bond breaking and yield an abnormal latent heat of vaporization. Thus a cyclic alcohol model is consistent with the observed behavior.

Still precise knowledge is lacking in the characterization of alcohols as polymeric structures. However, the alcohol structure is believed to be composed of two-dimensional linear polymers of varying lengths.[34]

C. Alcohol--Water Mixtures

The nature of alcohol and water structures are very complex, water structure being the most obscure of the two. Thus, an even more complex system is developed in mixtures of alcohol and water. However, some general actions have been made in the quest to find out what water is really like. Franks and Ives have used thermodynamic excess functions of mixing in alcohol--water systems. The thermodynamic excess functions' dependence on temperature has been observed over a three-temperature range: 25°, 50°, and 75°C. The free energy (Figure 1) shows the least amount of change, and may be considered independent of temperature. The increase in the enthalpy and entropy terms as the temperature changes indicates a steady decrease in hydrogen bonding and a decrease in structure resulting in an increase in the entropy, ΔS. A nonhydrogen bonding species, dioxane, and a hydrogen bonding species tert-butanol were combined with water to form binaries which have been studied using the thermodynamic functions of mixing. The systems dioxane--water and tert-butanol--water can be compared (Figures 2 & 3). There is no

FIGURE 1. VARIATION WITH TEMPERATURE OF THE EXCESS FUNCTIONS OF THE ETHANOL--WATER SYSTEM

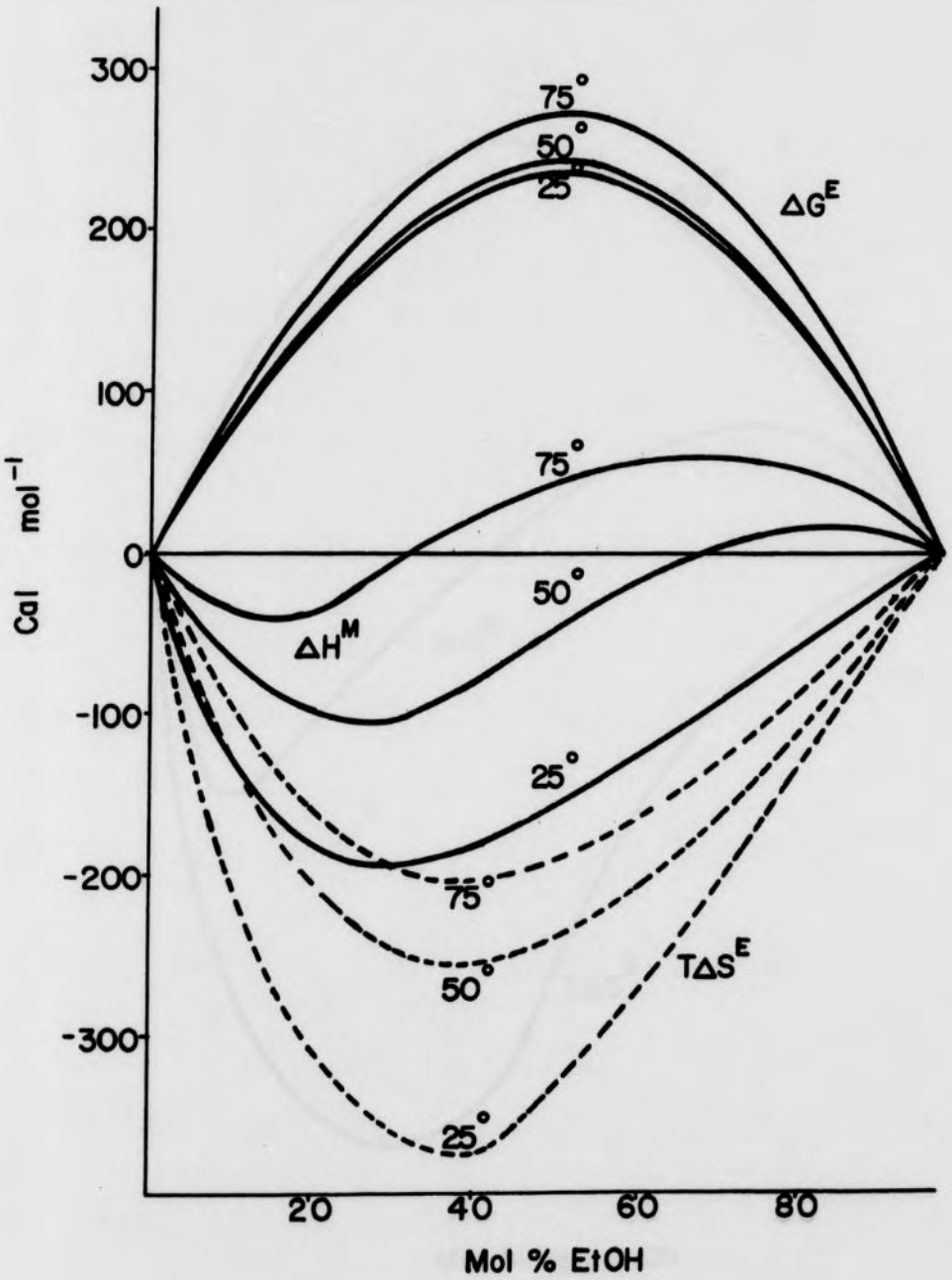

FIGURE 2. THERMODYNAMIC EXCESS FUNCTIONS FOR THE TERT-BUTANOL--WATER SYSTEM AT 25°C

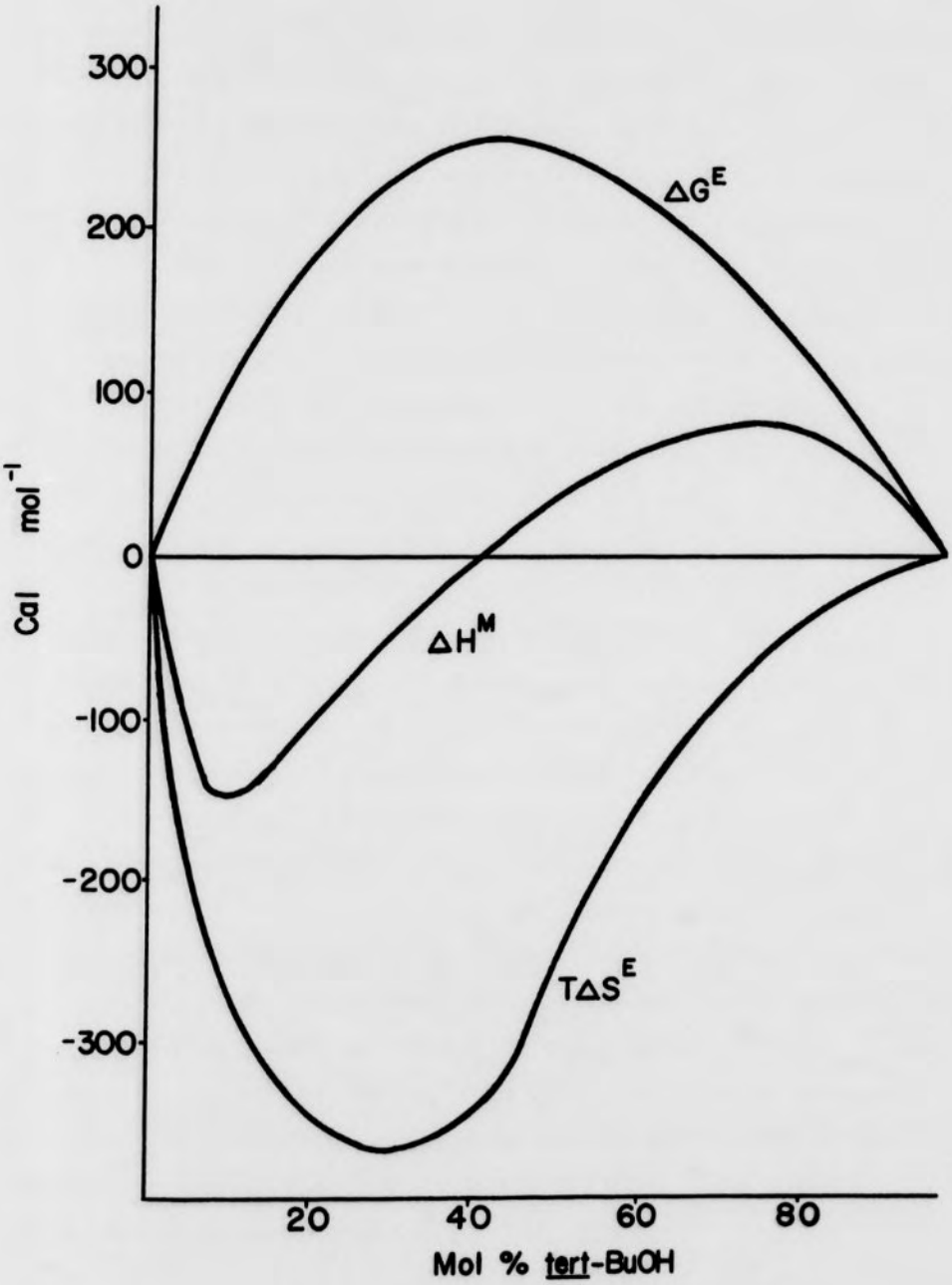

FIGURE 3. THERMODYNAMIC EXCESS FUNCTIONS FOR THE DIOXANE--WATER SYSTEM AT 25°C

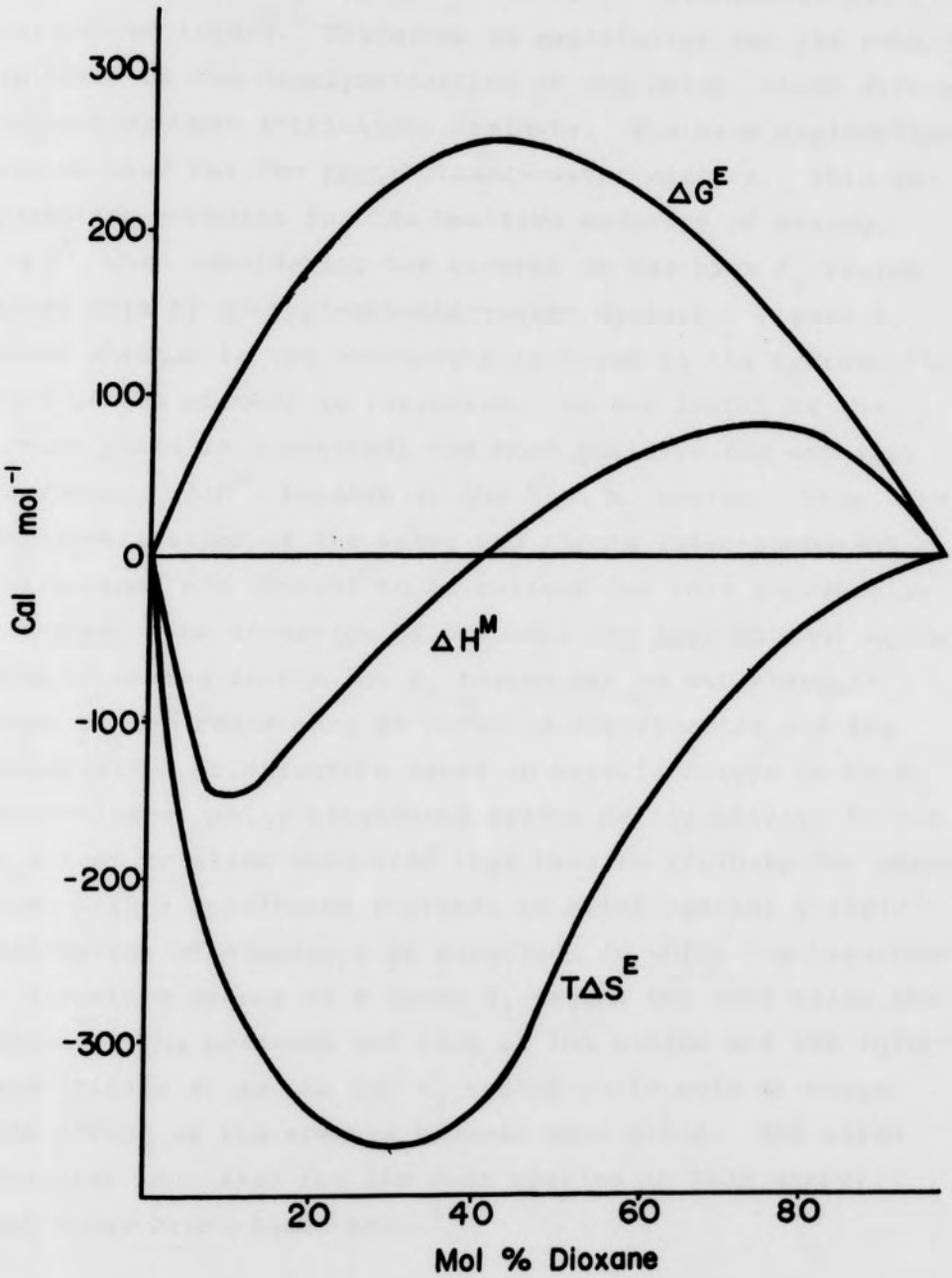

visible difference between these two solvent mixtures in terms of their thermodynamic functions. Dioxane is not a structured liquid. Therefore an explanation for its behavior is based on the depolymerization of the water, where strong inter-component attractions dominate. The same explanation can be used for the tert-butanol--water mixture. This explanation accounts for the positive enthalpy of mixing, ΔH^M, when considering the alcohol in the high X_2 region ($\sim$80 mole %) of tert-butanol--water mixture. Figure 4 shows changes in the thermodynamic terms as the hydrophobic part of the alcohol is increased. As the length of the carbon chain is increased, the more positive the enthalpy parameter, ΔH^M, becomes in the high X_2 region. Thus, the depolymerization of the water and strong inter-component attractions are thought to be reasons for this increase in enthalpy. The inversion of propanol and tert-butanol enthalpies of mixing in the low X_2 region can be explained in terms of the resistance of water to depolymerize and the preservation of structure based on water's nature to be a three-dimensionally structured system or its ability to act as a host to alien molecules that have an affinity for water. Thus, with a continuous increase in alien species a rapid destruction of structure is expected, in which the breakdown in structure occurs at a lower X_2 region the more alien the invader. The position and size of the minima and the inversion (Figure 4) in the low X_2 region ($\sim$10 mole %) shows this effect as the species becomes more alien. The alien character increases for the four species in this manner: tert-BuOH> PrOH> EtOH> MeOH.[34]

FIGURE 4. HEATS OF MIXING (ΔH^M) WITH WATER AT 25° OF METHANOL, ETHANOL, N-PROPANOL, AND TERT-BUTANOL

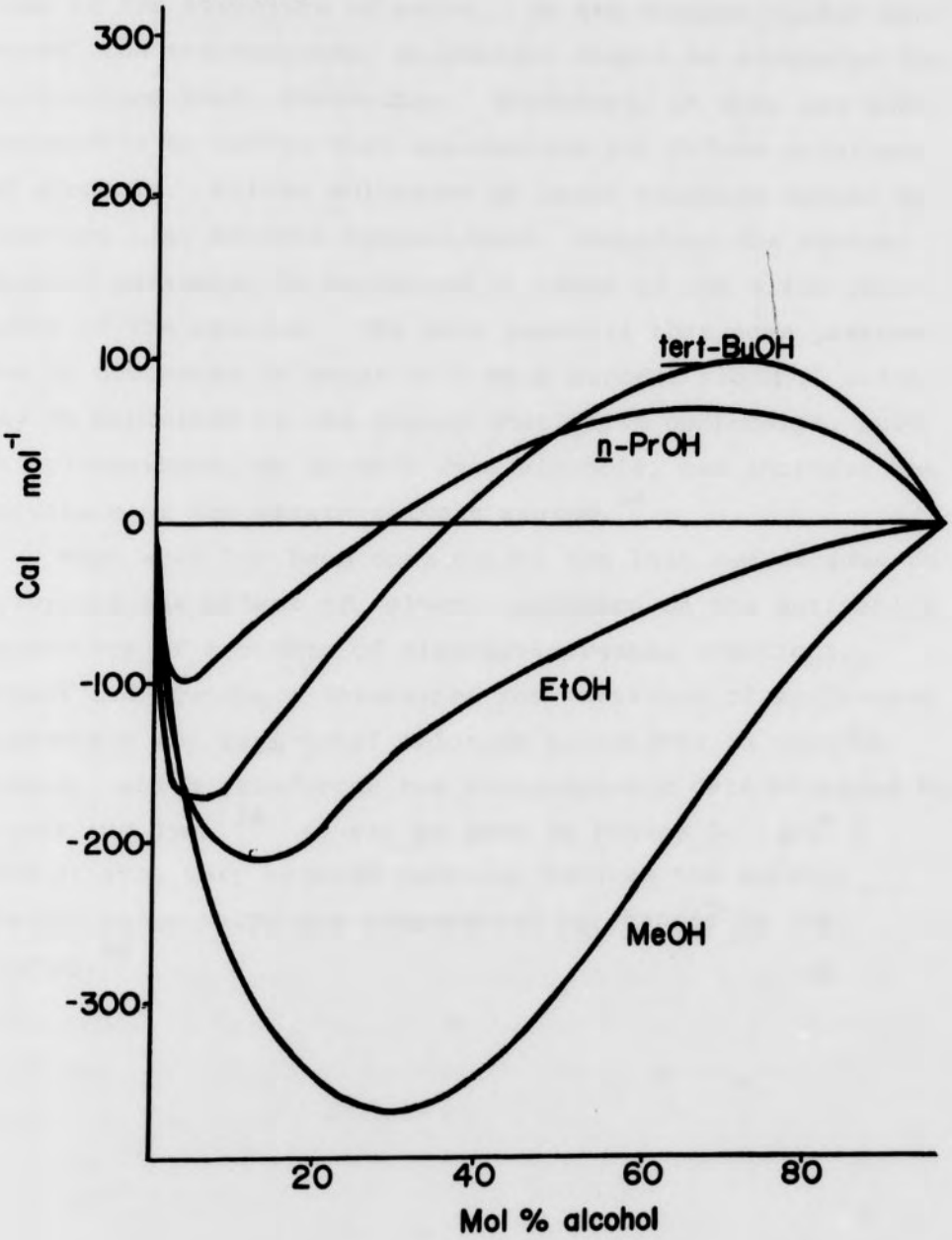

The large negative excess entropies of mixing as observed in Figures 1, 2, and 3 do not suggest a general breakdown in the structure of water. In the dioxane--water mixtures, the thermodynamic parameters cannot be accounted for by hydrogen bond interaction. Therefore, it does not seem reasonable to invoke that explanation for dilute solutions of alcohols. Dilute solutions of large alcohols appear to function like soluble hydrocarbons, therefore the thermodynamic parameter is explained in terms of the alien character of the species. The main point is that some phenomenum is occurring at about 5-10 mole percent alcohol, which may be explained by the theory that alien components, such as hydrocarbons, or in this case alcohols, can increase the structure of the water--solvent system.[34]

Much work has been done during the last two decades to determine the effect of solvent variation on the activation parameters of a number of classical-organic reactions. Arnett and coworkers determined the variation of activation parameters for tert-butyl chloride solvolysis in aqueous ethanol, which reinforces the thermodynamic data obtained by Franks and Ives.[34] As can be seen in Figure 5, (ΔG^{*}) demonstrates very ordered behavior because the erratic changes in enthalpy are compensated by changes in the entropy.[44]

Figure 5. Variation of Activation Parameters

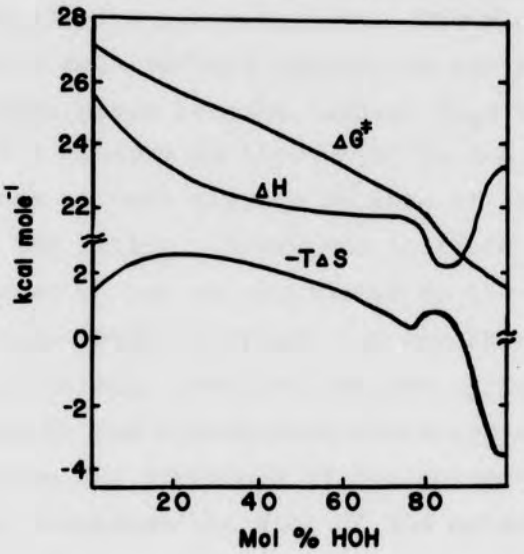

Arnett has used other continuously varied compositions of binary solvents and gradually perturbed the reaction mechanism to learn more about activation parameters. However, instead of increasing the understanding of solvent properties with respect to the activation parameters, his studies have revealed new dimensions leading to more confusion concerning water solvent mixtures.[34]

Additional functions that show alcohol--water solvent mixture characteristics are velocity of sound and sound absorption coefficients in the mixture of water with ethanol and water with tert-butanol. These show maxima in the same 5-10 mole percent alcohol region. These maxima are also thought to indicate a more compact and structured water molecule.[45]

Partial molal volumes in alcohol--water mixtures show a minimum for the alkylammonium cations. The minimum appears in the 5-10 mole percent region and its size increases as the alkyl group becomes larger, $Me_4N^+ < Et_4N^+ < Pr_4N^+ < Bu_4N^+$. This minimum is thought to be due to a structural change in the solvent mixture because of the hydrophobic nature of the cation. A maximum is found at about 0.3 mole fraction which can be attributed to the size effect.[46] Partial molal data by Franks and coworkers show the minimum at about 0.05 mole fraction for the tert-butanol--water mixture, due to the hydrophobic character of the butyl group which promotes the structure of the solvent. A temperature increase decreases the size of the minimum and moves it to a lower mole percent, the amount of shift depending on the amount of temperature change. These data reinforce the structural change explanation in that as the temperature is increased the structure is probably decreased; thus it would be expected that the extrema characteristics would decrease and occur at a lower mole fraction. Franks has shown an extremum point in the water--alcohol mixtures by using the first derivative plots of viscosity, (η) versus mole percent alcohol. For the first derivative curve ($d\eta/dc$), the change in viscosity with respect to concentration shows a maximum at about 10 mole percent, where the maximum structuredness of the ethanol--water solvent mixture occurs.[47] Frank and Wen have observed that the heat capacity of alcohol--water mixtures increases in the same way as for aqueous alkylammonium salt solutions. The maximum which appears at approximately 0.1 mole fraction alcohol has been attributed to the increase in the structure of the solvent

because of the hydrophobic nature of the species added to the alcohol--water system.[11] Conductance data for HCl in the methanol--water solvent mixture also exhibits a similar maximum in the same region. Structure changes of the solvent system have also been invoked to explain this extremum characteristic.[48] The transition energy, E_t, for the composition curve for tert-butanol--water solutions of a merocyanine dye undergoes a sharp reversal at about five mole percent alcohol in the alcohol--water mixture. This inversion has also been attributed as a result of the point where the solvent system was at its greatest structuredness.[49]

Arnett and coworkers have done an extensive amount of work on the solvent effects of many hydrocarbons and hydrocarbon salts in alcohol--water solvent systems. They investigated systems such as methanol--water, sec-butanol--water, tert-butanol--water, DMSO--water, dioxane--water, and acetone--water. They also studied binary systems in which water was not one of the components.[35] They generally selected a series of solutes to study such as alkylammonium chloride salts (Me_4NCl, Et_4NCl, Pr_4NCl, and Bu_4NCl), or the halogen series (KCl, KBr, and KI). The heats and entropies of solution in all these alcohol--water mixtures studied show the same phenomena as mentioned above -- a maximum at about 5-10 alcohol mole percent. These phenomena were also explained by Arnett as the point at which water was most structured. At points before the extremum point the introduced alien is thought to promote structure in the water part of the system. At points after the extremum point the excess alien begins to rupture and destroy the water structure.[35]

Arnett has also used kinetic, thermodynamic and spectral behavior of a variety of other solutes in his study of organic--aqueous systems which revealed an extremum at about a 1:17 mole ratio of tert-butanol to water. This mole ratio has been suggested as a point of clathrate structure formation. Clathrate structures are cagelike species with, in this case, one alcohol molecule surrounded by 17 water molecules or some small whole number multiple.[35] X-ray crystallography studies at 70°C indicate that the formation of clathrate structures for acetone, dioxane, and ethanol occurs in an organic--aqueous solvent system having a mole ratio of 1:17.[50] It is interesting that dioxane and tert-butanol have exhibited identical thermodynamic properties of mixing in organic-aqueous solvent studies done by Frank and Ives. At the present time, X-ray studies have not been done on the tert-butanol--water solvent system. Organic components other than tert-butanol in aqueous binaries reveal extremum at a 1:8 or 1:9 mole ratio of organic component to water. Arnett and Franks have explained this as an increase in the structuredness of water, indicating that the hydrogen bond formation has increased.[34,35]

This background of information shows remarkable phenomena in the behavior of alcohol--water systems, from a wide diversity of thermodynamic, kinetic, spectral, and other physical properties. The extrema generally appear in the 5-10 mole percent alcohol region of the alcohol--water solvent mixture. Many facts and trends have been extracted from these extrema, resulting from varying degrees of structuredness of the binary systems.

D. Hydrophobic and Hydrophilic Nature of Ions

Just as the added species described previously have been found to alter the structure of water, ions have now been labelled as structure makers (hydrophobic species) or structure breakers (hydrophilic species). Li^+ and F^- seem to be the only hydrophilic ions which are not structure breakers. This unique behavior is usually credited to the Li^+ and F^- high charge density (small size). Their high charge density increases water structure, and their small size does not disrupt the structure of the water very much. Alkali metals show the following trend: $K^+ > Na^+ > Li^+$ in structure breaking ability. Halogens show the trend $I^- > Br^- > Cl^- > F^-$ in structure breaking ability, with Li^+ and F^- being structure makers, as mentioned.[51] Alkylammonium chloride salts show the following trend: $Bu_4NCl > Pr_4NCl > Et_4NCl > Me_4NCl$ in structure making ability. Alcohols show the following trend: tert-BuOH > n-PrOH > MeOH, which indicates, as for the R_4N^+ salts, that as the length of the hydrocarbon chain increases the species becomes more structure making. This trend is attributed to an increased hydrophobic nature, mainly to its increase in size. Of course this applies only for alcohols which are water soluble.[32] The exact effect of phenyl groups has not yet been established. Compounds such as Ph_4PCl, Ph_4AsCl and $NaBPh_4$ seem to show both structure breaking and structure making properties, depending on the type of studies made. Kalfoglow and Bower have reported that based on osmotic and activity coefficients some of these salts would be structure breakers in water.[52] Millero has shown Ph_4AsCl as a structure-breaker, based on his partial molar volume

studies.[53] Mohanty and Ahluwalia have indicated these salts show no distinction in gross structure making or breaking abilities, based on partial molar heat capacity changes, ΔC_p^o.[54] Perron and Desnoyers concluded, using partial volume data, that salts containing phenyl rings were structure makers.[55] The structures of these compounds indicate that they should be structure makers because of their seemingly hydrophobic nature and size. The problem appears to be that the effect of the π electrons on the overall structure altering tendencies is not known. It is fairly certain, for example, that cyclohexane would be a structure making moiety, but it is not known for sure what effect benzene has on water structure. No convincing argument has yet been made, however, as to the actual status of these salts concerning their structure making or breaking characteristics.

Tremendous advances, as indicated by the data and theories presented in the previous sections have been made in the last ten years in the quest to explain the nature of liquid water. The explanations, theories, conclusions, and proposed models for liquid water will have to withstand the test of time, which means that much more data and experimental evidence will be required.

III. RESEARCH PROPOSAL

Thermodynamic and other properties have been used extensively by Franks, Arnett and others in the study of water structure. Franks and Ives have reported in their review of water--alcohol mixtures that when properties such as thermodynamic excess functions of mixing, partial molar volumes, and viscosity are plotted *versus* alcohol mole fractions, extremum appear in the highly aqueous region of the curve. Arnett has used heats of solution data (ΔH_s) *versus* alcohol mole fraction in the same way. Both men have concluded from independent research programs that the extrema exhibited by plots of the above functions *versus* alcohol mole fractions are indicative of an increase in the structuredness of water caused by the alcohol nonelectrolyte.

In this research project thermometric precipitation titrations of slightly soluble salts are proposed as another method to study water structure. The enthalpy of the precipitation reactions will be obtained at various water--alcohol concentrations to determine if extremum in the enthalpy *versus* alcohol mole fractions plot results at the position of known maximum structuredness as found by Franks and Arnett. Precipitation reactions will be investigated because it is desirable to have a series of simple, straightforward, well characterized probe reactions for use in the study of other organic--aqueous solvent mixtures. A better understanding of the effects of various nonelectrolytes on chemical reactions and on water should result from studies such as these. In addition data obtained in this research may be useful for

relating the size of the extrema to the overall relative structure making or breaking abilities of the ions involved. Since tetraphenylarsonium and tetraphenylborate precipitation reactions will be studied, the results may possibly resolve the question of whether phenyl groups are structure makers or breakers as discussed in the Historical Background section. Lastly, the data in this research will then be available to test, if possible, present and future water model structures. It will be necessary that any model suggested must be consistent with all reliable data, this work included.

An extremum is expected for the precipitation probe reactions in the plot of the measured enthalpy, ΔH^{o}, versus the percentage of tert-butanol in the solvent system. The precipitation process has several contributing factors. The heat of desolvating the ions, an endothermic condition, indicates that energy is necessary to expose the anion and cation. With the ions exposed molecular formation will take place, which results in an exothermic contribution. The heat of crystallization is released as the molecules become further exposed and begin to gather and precipitate. The heat of crystallization is probably an exothermic contribution. The overall enthalpy measured is comprised of the four heat contributions, mentioned above, plus any heat term which results from structure changes in the solvent system upon precipitation. Infinite dilution is assumed in the expression as all concentrations are to be millimolar. The overall measured enthalpy change can be stated as:[51]

$$\Delta H^{o} = \Delta H^{o}_{a} + \Delta H^{o}_{c} + \Delta H^{o}_{f} + \Delta H^{o}\ \text{cryst.} + \Delta H^{o}_{st} \qquad \text{Eq. 3}$$

where,

ΔH^{o} is the overall measured enthalpy.

ΔH^{o}_{c} is the heat of desolvation of the cation.

ΔH^{o}_{a} is the heat of desolvation of the anion.

ΔH^{o}_{f} is the heat of formation of cation--anion molecules.

ΔH^{o} cryst. is the heat of crystallization.

ΔH^{o}_{st} is the heat resulting from any structure change in the solvent system.

The heats of formation and crystallization in the expression are essentially proportional to the lattice energy of the solid.

The heats of transfer, $\Delta H^{o}_{tr,}$ from a mixed solvent to pure water are obtained by subtracting the overall ΔH^{o} of the reaction in pure water from the overall ΔH^{o} of the reaction in a solvent mixture and is given by the following expression:

$$\Delta H^{o}_{tr} = \Delta H^{o}_{(mix)} - \Delta H^{o}_{H_2O} \qquad \text{Eq. 4}$$

Substituting in all heat quantities of Eq. 2 into Eq. 4 for both $\Delta H^{o}_{H_2O}$ and ΔH^{o}_{mix}

$$\Delta H^{o}_{tr} = \left\{\Delta H^{o}_{a(mix)} - \Delta H^{o}_{a(H_2O)}\right\} + \left\{\Delta H^{o}_{c(mix)} - \Delta H^{o}_{c(H_2O)}\right\} \qquad \text{Eq. 5}$$
$$+ \left\{\Delta H^{o}_{f(mix)} - \Delta H^{o}_{f(H_2O)}\right\} + \left\{\Delta H^{o}_{\text{cryst.}(mix)} - \Delta H^{o}_{\text{cryst.}(H_2O)}\right\}$$
$$+ \left\{\Delta H^{o}_{st(mix)} - \Delta H^{o}_{st(H_2O)}\right\}$$

The heats, $\left\{\Delta H^{o}_{a(mix)}, \Delta H^{o}_{a(H_2O)}\right\}$ and $\left\{\Delta H^{o}_{c(mix)}, \Delta H^{o}_{c(H_2O)}\right\}$ resulting from the desolvation of the anions and cations should be equal or nearly so in the highly aqueous region, from 0 to 10% tert-butanol. It is assumed that in this

region of the binary solvent system the ions are only solvated by water molecules, because of the small size of water compared to tert-butanol and also because of the preponderance of H_2O molecules. In addition, the steric effect of the bulky butyl groups of the tert-butanol should seriously limit the solvating of the ions by these molecules. Hence, these desolvation terms are assumed to be virtually cancelled in the ΔH^{o}_{tr} expression as mentioned above. The heat of formation of cation--anion molecules, ΔH^{o}_{f}, and the heat of crystallization, ΔH^{o}_{cryst} are assumed to be constant and independent of the solvent medium. Thus, they also cancel out in ΔH^{o}_{tr}; therefore, the heats of transfer from solvent mixture to pure H_2O, as stated in the following expression

$$\Delta H^{o}_{tr} - \Delta H^{o}_{st(mix)} - \Delta H^{o}_{st(H_2O)} \qquad \text{Eq. 6}$$

is indicative of structure changes caused by the tert-butanol in the water. It would be naive to equate ΔH^{o}_{tr} solely to structural effects, since there may well be other factors that contribute to the overall measured enthalpy but are not cancelled. But it is assumed here that these heats are small with respect to that heat resulting from structure changes.

Therefore, for these probe reactions to be useful in the study of other aqueous solvent binaries reasonably large extrema need to be exhibited. The extrema in ΔH^{o}_{tr} should occur at a ratio of approximately 5% alcohol in tert-butanol solvent mixtures, as was found for the measurements in tert-butanol--water by Franks and Arnett.[31,32]

IV. THEORY OF THERMOMETRIC TITRATIONS

A. Thermometric Titrations

Thermometric titrations are normally done under adiabatic conditions in which the temperature change of a reaction (ΔT) is plotted against the volume of titrant consumed {or the time (Δt)}. These plots or titrations curves are called enthalpograms.[57] The power of this method was limited during its early development by poor instrumentation, which led to results with poor accuracy and precision. However, innovations and automations in the adiabatic, as well as the development of nonadiabatic systems, have tremendously increased the potential use of thermometric titration systems as good analytical techniques.

Bell and Cowell first suggested that heats of reaction could be used as a new analytical method in 1913.[58] However, it was not until 1922 when Dutoit and Grobet applied enthalpimetric titrations to neutralization reactions, precipitations, and complexations that the scope of such a method was realized.[59] At that time, mercury thermometers were used as the temperature sensors. The large response lag of the mercury thermometer caused large errors and much inconsistency in the data. This problem was essentially eliminated in 1953 when Hume and coworkers revolutionized the method by introducing thermistors as the temperature sensing probe. The response lag of thermistors is about one second or less. Thus, the precision and accuracy of the method was greatly improved.[60] Other improvements were incorporated into the system in a short

time which also improved the accuracy and precision and increased the credibility of the method. For instance, Jordan and coworkers used an automatic buret in 1957 which mechanized the system further, thus decreasing the human error.[61] Also, the advent of the differential system by Tyson, McCurdy, and Bricker in 1961 marked a significant advance because extraneous heats were eliminated by the electrical circuity.[62] Eatough, Snow, and Christensen adapted their apparatus to a computer which allowed the experimenter to go from the initialized system to the calculated enthalpogram and a readout of the results desired in a very short period of time.[63] Then in 1962, the status of the method was so established that the American Instrument Company produced the first commercial instrument.[64] This was followed by further automation by Priestley who used an automatic digital thermometric titrator.[65] Another step in the advancement of the thermometric titration system was made by Smith, Barnes, and Carr who used a lock-in amplifier and a linear ramp generator system. They were able to obtain temperature resolution of 3-4 $\mu^{\circ}C$ and were able to utilize very low concentration levels for the titrant and titrand (15 μM). The precision was 0.2% when measuring in the range of 20 mcal of heat or more for the titration and with concentrations as low as 1.5 mM. The precision was limited to the error in the flow rate measurement of the syringes. The accuracy of the data obtained by Smith, Barnes, and Carr was also excellent.[66]

The improvements on adiabatic thermometric titrations was followed by the development of various thermometric techniques based on nonadiabatic conditions. In a

nonadiabatic system, heat is exchanged freely between the reaction vessel and the environment. Problems still exist, however, which must be solved in order to gain full use of the system. As in an adiabatic system, heat leakage presents a serious problem. However, in the nonadiabatic system the heat leakage problem is reduced because heat accumulation is decreased.[67] The nonadiabatic system is best adapted to reactions that evolve heat at slow rates. This reduces the amount of heat accumulated in the sample cell and in return reduces the chance for heat leak. The temperature changes of the solutions follow Newtonian behavior so closely that the thermal phenomena can be treated mathematically. Endpoint determinations present another problem in the nonadiabatic system. The use of analog computer technique is necessary to determine the endpoint of a reaction. However, this technique shows promise as a method as more innovations eliminate its deficiencies.[67]

Another nonadiabatic system developed by Christensen, Johnson, and Izatt employs an isothermal titration calorimeter. The isothermal titration calorimeter uses a heater and a Peltier cooler to keep the reaction cell at the same temperature throughout the titration. The total heat of reaction (Q_R) measured is equal to the heat absorbed by the cooler (Q_C) minus the heat given out by the heating unit (Q_M).

$$Q_R = Q_C - Q_M \qquad \text{Eq. 7}$$

In actual practice the cooler is kept constant while the heating unit is controlled to maintain an isothermal condition. If an exothermic reaction is occurring, the amount

of heat supplied to the cell is decreased to compensate for the reaction. This decrease in heat supplied to the cell to maintain the isothermal condition is equivalent to the heat of reaction. This system is limited to slow reactions, which is an advancement in thermometric analysis since the adiabatic systems are limited generally to fast reactions to reduce heat leakage, which is not a problem under isothermal conditions.[68]

Direct Injection Enthalpimetry (DIE) was introduced by Wasilewski, Pei, and Jordan. The method requires the titrant to be injected in one second or less, the reaction must be practically instantaneous, and a rapid temperature recording system must be used. In this system the change in voltage, ΔE, must be recorded in 0.5 seconds after mixing. The technique is a comparison of the temperature change occurring upon the addition of excess titrant to a known volume of the unknown component with those of the calibration run. However, the calibration reactions must be run carefully in the region of the unknown concentration. Such systems are useful when the volume of determinations is large, as in a quality control lab where incoming and outgoing concentrations of various materials are analyzed.[69]

B. Mathematical Development of Differential Systems

Differential titration techniques, as developed by Tyson, McCurdy, and Bricker, are a significant advancement as mentioned previously. One advantage of using a differential system is that many extraneous heats may be cancelled systematically while these same heats must be corrected for mathematically in a nondifferential system, which is not easily done under some conditions and even impossible under

other conditions. Such heats as heat of dilution of the titrant, heats of stirring and thermistor heats are cancelled in the system when they are the same in both cells. Since the heats are equal and the arms of the Wheatstone bridge have the same response character, the heats are cancelled by the circuitry, and thus not reflected in the recorder trace. Therefore, the imbalance in the system can then be attributed solely to that caused by the overall enthalpy of the reaction. A second advantage of a differential system is that the shape of the enthalpogram obtained lends itself to direct calculations more easily than an enthalpogram of a nondifferential system.[62] (Figure 6)[70]

Figure 6. Differential and Nondifferential Enthalpograms
(a) Differential (b) Nondifferential

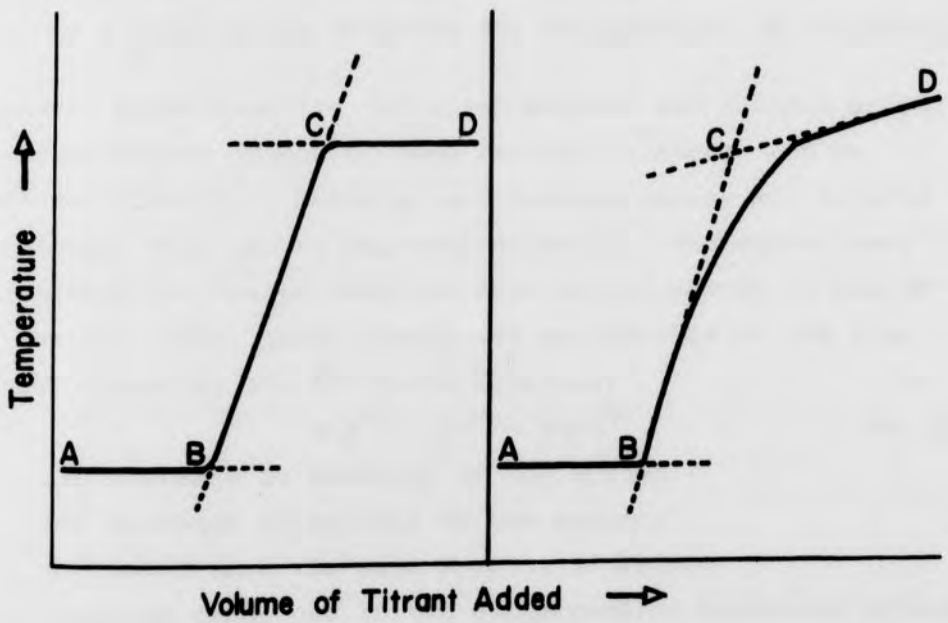

The breaks in the enthalpogram in diagram (a) are much more defined than in (b) making it easier to obtain accurate measurements. However, an excessive amount of time is often required to obtain an isothermal condition between the two cells in the differential system before a titration can begin. Still differential titration systems have been used extensively since 1961 and have been demonstrated to yield both accurate and precise data.[65]

Mathematically potentiometric titration methods are related to the free energy change during a reaction, or thermodynamically as,

$$\Delta G^{o} = - RT\ln K \qquad \text{Eq. 8}$$

ΔG^{o} = change in free energy.

R = universal gas constant.

T = temperature in degrees Absolute.

K = equilibrium constant for the reaction at temperature T.

However, potentiometric titration methods are useless unless the free energy change or some related parameter can be measured directly. Enthalpy and entropy values are related parameters that can be measured directly. Therefore these parameters are useful when the free energy cannot be measured easily. Also, these quantities are related to the free energy change by the following equation:

$$\Delta H^{o} = \Delta G^{o} + T\Delta S^{o} \qquad \text{Eq. 9}$$

ΔH^{o} = change in enthalpy of the system.

ΔS^{o} = change in entropy of the system.

ΔG^{o} and T have the same meaning as before.

This research makes use of the enthalpimetic titration method of analysis, which measures the temperature change,

ΔT, which is plotted against the volume of titrant, ΔV, used. Given a general reaction,

$$xU + yR \rightleftharpoons zP \qquad \text{Eq. 10}$$

the total heat (Q calories) of the reaction is related to the molar heat of the reaction, ΔH, by the expression:

$$Q = - n_p \Delta H \qquad \text{Eq. 11}$$

where n_p is the moles of product formed which is related to the change in temperature, ΔT, by:

$$Q = \underline{C}_p \Delta T \qquad \text{Eq. 12}$$

$\underline{C}_p$ being the heat capacity. As in the case of the direct injection enthalpimetric titrations, the titrant, R, must be added in excess so that the reaction will proceed to virtual completeness. At this point the following relation will exist:

$$n_R^i << (y/x) n_u^i \qquad \text{Eq. 13}$$

Thus,

$$n_u^i U + n_R^i R \longrightarrow \left\{ z/x\ n_u^i P + \left(n_R^i - y/x\ n_u^i \right) R \right\} \approx \qquad \text{Eq. 14}$$

$$\left\{ n_p P + \left(n_R^i - y/z\ n_p^i \right) R \right\}$$

where n_R^i represents the number of moles of excess titrant, n_u^i represents the moles of an unknown initially present, and the expression represents the final product. The above condition also implies that,

$$n_p \approx (z/x) n_u^i \qquad \text{Eq. 15}$$

Such conditions depend on the equilibrium constant of the reaction. By equating Equation 15 and Equation 11,

$$Q = -(z/x) n_u^i \Delta H \qquad \text{Eq. 16}$$

and by rearranging Equation 12,

$$\Delta T = Q/\underline{C}_p \qquad \text{Eq. 17}$$

Substitution of Equation 16 into Equation 17 yields:

$$\Delta T = -(z/x)n_u^i \Delta H/\underline{C}_p \qquad \text{Eq. 18}$$

Under ideal conditions the enthalpy value, ΔH, will approach a constant value, therefore, ΔH times $-(z/x)$ is to a constant.

$$k = -(z/x)\Delta H = \text{const.} \qquad \text{Eq. 19}$$

Thus Equation 20 can be obtained by substituting Equation 19 into Equation 18 and combining the constants.

$$\Delta T = \text{constant } n_u^i \qquad \text{Eq. 20}$$

Thus, Equation 20 gives the linear relationship of the enthalpograms. By plotting temperature change, ΔT, of the reaction against moles of titrant, (n_u^i), both can be measured directly, thereby making thermometric titration systems possible.

Mathematical equations are also used to describe the thermometric titration curves. Figure 7[64] shows examples of both exothermic and endothermic enthalpograms. Thermometric titration curves are ultimately plots of temperature <u>versus</u> time. Because the titrant is delivered at a constant rate, the following relationships exist:

$$dv/dt = a = \text{constant} \qquad \text{Eq. 21}$$

$$v_t = v_o + at \qquad \text{Eq. 22}$$

where a is the flow rate constant for the titrant, v_t the volume of titrant used at time t, and v_o the volume at $t = 0$. The system is assumed to be an ideal adiabatic system and a system where the kinetics of the reaction are fast enough to allow the reaction to go to completion in the time allotted for the titration. Heat flux of the reaction can be calculated by Equation 23.

FIGURE 7. TYPICAL ENTHALPOGRAMS

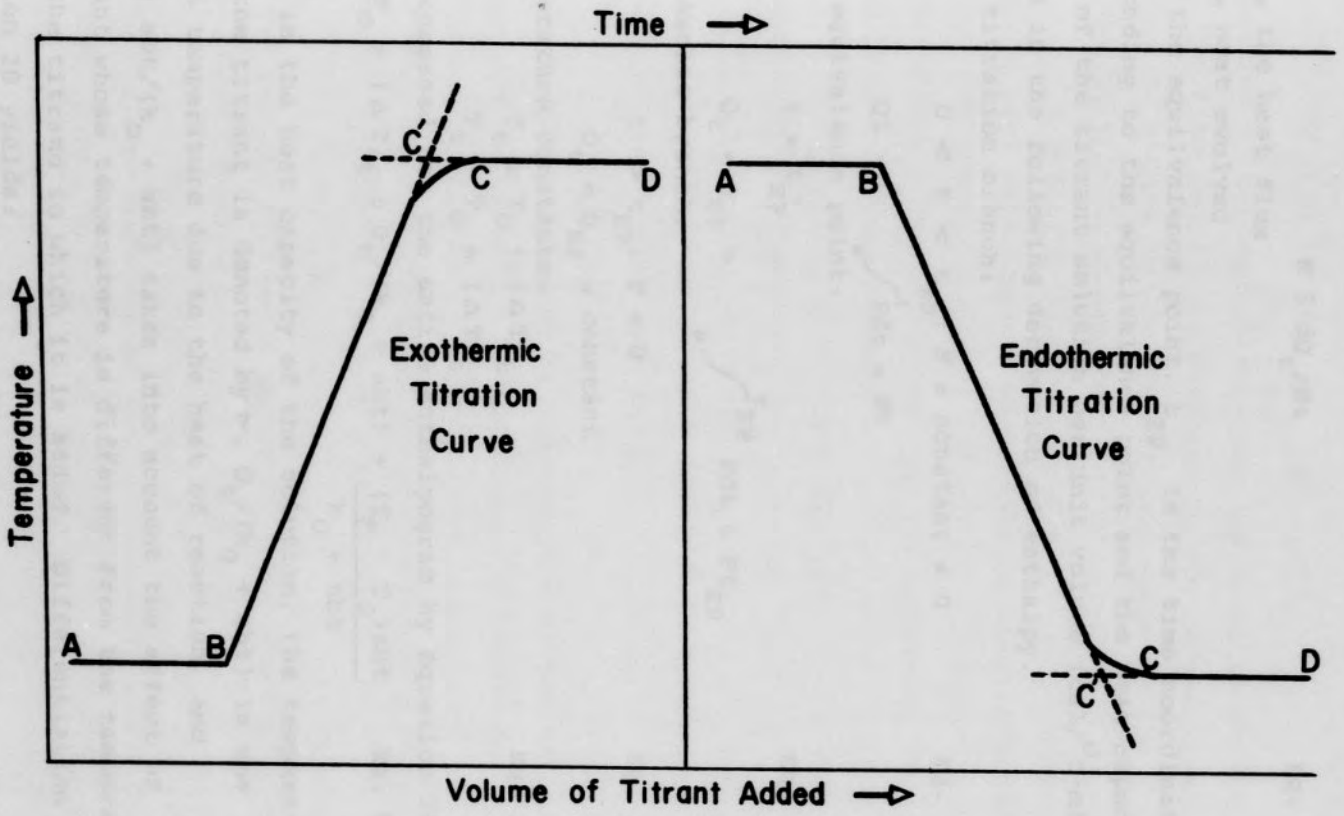

$$F \equiv dQ_t/dt \qquad \text{Eq. 23}$$

F = the heat flux

Q = heat evolved

Time at the equilvalence point, $t_{EP,}$ is the time coordinate corresponding to the equilvalence point and the heat capacity, b, of the titrant solution per unit volume (cal/^{o}C-ml) are used in the following derivation of enthalpy.

For the titration branch:

$$0 < t < t_{EP};\ F = \text{constant} \neq 0 \qquad \text{Eq. 24}$$

$$Qt = \int_{o}^{t} Fdt = Ft$$

For the equivalence point:

$$t = t_{EP} \qquad \text{Eq. 25}$$

$$Q_t - Q_{EP} = \int_{o}^{t_{EP}} Fdt = Ft_{EP}$$

For the excess branch:

$$t > t_{EP};\ F = 0 \qquad \text{Eq. 26}$$

$$Q_t = Q_{EP} = \text{constant}$$

The temperature constants:

$$T_t = T_o + (\Delta T)_t \qquad \text{Eq. 27}$$

$$T_t - T_o = (\Delta T)_t$$

can be expressed for the entire enthalpogram by Equation 28.

$$T_t - T_o = (\Delta T)_t = Q_t/(k_o + abt) + \frac{(T_\tau - T_o)abt}{k_o + abt} \qquad \text{Eq. 28}$$

Where k_o is the heat capacity of the solution, the temperature of the titrant is denoted by τ, $Q_t/(k_o + abt)$ is the change in temperature due to the heat of reaction, and $(T_\tau - T_o)\ abt/(k_o + abt)$ takes into account the effect of the titrant whose temperature is different from the temperature of the titrand to which it is added. Differentiation of Equation 28 yields:

$$\frac{d(\Delta T)_t}{dt} = \frac{(T_r - T_o)\, ab + Ft}{k_o + abt} \qquad \text{Eq. 29}$$

Thus, Equation 28 represents the line and Equation 29 the slope of the line describing the portion BCD of the titration curves in Figure 7. If the concentrations of the titrant are relatively large then:

$$(\Delta v)_{EP} \equiv (v_{EP} - v_o) << v_o \qquad \text{Eq. 30}$$

A negligible heat capacity can be assumed in view of Equation 30 and therefore:

$$abt << k_o;\ (k_o + abt) \approx k_o = \text{a constant} \qquad \text{Eq. 31}$$

Equations 28 and 29 then become,

$$(\Delta T)_t = 1/k_o \{Q + (T_r - T_o)\, abt\} \qquad \text{Eq. 32}$$

for the enthalpograms, and,

$$\frac{d(\Delta T)}{dt}_t = 1/k_o \{F_t + (T_r - T_t)\, at\} \qquad \text{Eq. 33}$$

for the slope of the enthalpogram. Under these conditions the assumption also can be made that:

$$(T_r - T_o)\, abt << Q \qquad \text{Eq. 34}$$

because the slight difference in temperatures of the titrant and titrand are negligible. In addition, the sample and blank cells are subjected to the identical temperature changes. Thus, in a differential system temperature differences cancel. Equation 28 is then simplified to:

$$(\Delta T)_t = Q/k_o \qquad \text{Eq. 35}$$

which is the general relationship for an ideal thermometric titration. From Equation 29,

$$\Delta T = -\Delta H C_R / k_o \qquad \text{Eq. 36}$$

where C_R is the concentration of the titrant in Equation 36. The titration slope, derivative of Equation 36, is taken with respect to time and volume as they approach zero. The titration slope equals:

$$\frac{(dT)}{(dt)_{t \rightarrow 0}} = a(dT/dv)_{v \rightarrow 0} = -a\ \Delta HC_R/k_o \qquad \text{Eq. 37}$$

The instrument is calibrated by introducing in a linear fashion a known amount of heat via a calibration heater. The calibration slope is calculated from current and resistance measurements of the apparatus. Therefore, the calibration slope is:

$$(dT/dt) = i^2R/4.185\ k_o \qquad \text{Eq. 38}$$

where i is the current supplied to a calibration heater, R is the resistance of the heating coil and k_o is the heat capacity constant for the solution. By combining Equations 37 and 38, the equation is obtained for the calculation of the enthalpy of the reaction. The equation is:[71]

$$\Delta H = \frac{i^2R}{4.185a} \times \frac{1}{C_R} \times \frac{\text{titration slope}}{\text{calibration slope}} \qquad \text{Eq. 39}$$

Tyson, McCurdy, and Bricker made use of the product of the two voltages across the heating coil and across the standard resistor, and the resistance of the standard resistor instead of using the current through the heating coil. The equation for the calculation of the enthalpy of a reaction takes the following form:[62]

$$\Delta H = E_1E_2S_1/4.185\ RNS_2 \qquad \text{Eq. 40}$$

E_1 is the voltage across the heating coil.

E_2 is the voltage across the standard resistor.

R is the resistance of the standard resistor in ohms.

N is the normality of the titrant in eq/liter.

F is the flow rate of the buret in ml/sec.

S_1 is the slope of the titration curve.

S_2 is the slope of the heating curve or the calibration slope.

C. Applications

When the enthalpy, ΔH, has been calculated from the thermometric titration data and the equilibrium constant is known, the entropy and free energy parameters can be determined from the following equalities:[64]

By definition, $$\Delta H \approx \Delta H^{\circ} \qquad \text{Eq. 41}$$

$$\Delta S^{\circ} = \frac{\Delta H^{\circ} - \Delta G^{\circ}}{T} = \frac{\Delta H^{\circ} + RT\ln K}{T} \qquad \text{Eq. 42}$$

ΔS° = entropy.

ΔH° = enthalpy.

ΔG° = free energy

T = temperature in $^{\circ}A$

R = universal constant

K = equilibrium constant

The stoichmetric relationships can be determined from endpoint determinations coupled with the concentration of either the titrant or titrand. Concentration of an unknown can be determined for situations where some type of continuous monitoring is necessary. Thus thermometric titrations are a valuable analytical tool in this respect. Thermometric titrations have also been used in basic research for various studies such as that done in this research project.

D. Precision of Thermometric Titrations

The precision of the enthalpy values obtained by thermometric titrations depends on the information desired. For analytical endpoint determinations the precision obtained has been 1% or better.[62,72,73] However, somewhat poorer precision is usually obtained when enthalpies are calculated. Systems that use specially designed Dewar flasks as cells

and where endpoint determinations are desired have resulted in a precision of 0.2%.[66] A commercially available titration calorimeter is the Titra Thermo Mat developed by Aminco. This instrument is capable, with extreme care, of reproducing data with about 1% precision.[74]

In this research, the 'initial slope' method of calculation has been employed to calculate the enthalpograms. This method attempts to correct for the change in heat capacity and heat leakage by using the initial slope of the enthalpogram. Line BC' (Figure 8) is extrapolated to zero titrant. Thus the heat capacity used in the final calculations is equivalent to the heat capacity of the initial system before the titration occurred. Enthalpy values obtained by this method have a reported precision between 2% and 10%.[75] Even though this method is rapid and theoretically accurate, it is extremely difficult to evaluate initial slopes with good precision unless adiabatic conditions are excellent. In this research only relative values of enthalpy were sought to investigate trends and maxima in the heats of transfer. In any case the selective discarding of enthalpograms that appeared to result from extraneous influences increased the precision to about 1%. Thus, the use of a relatively poor adiabatic system coupled with the 'initial slope' method did not significantly affect the results of this work.

FIGURE 8. ENTHALPOGRAM: SHOWING 'INITIAL SLOPE' METHOD OF CALCULATION

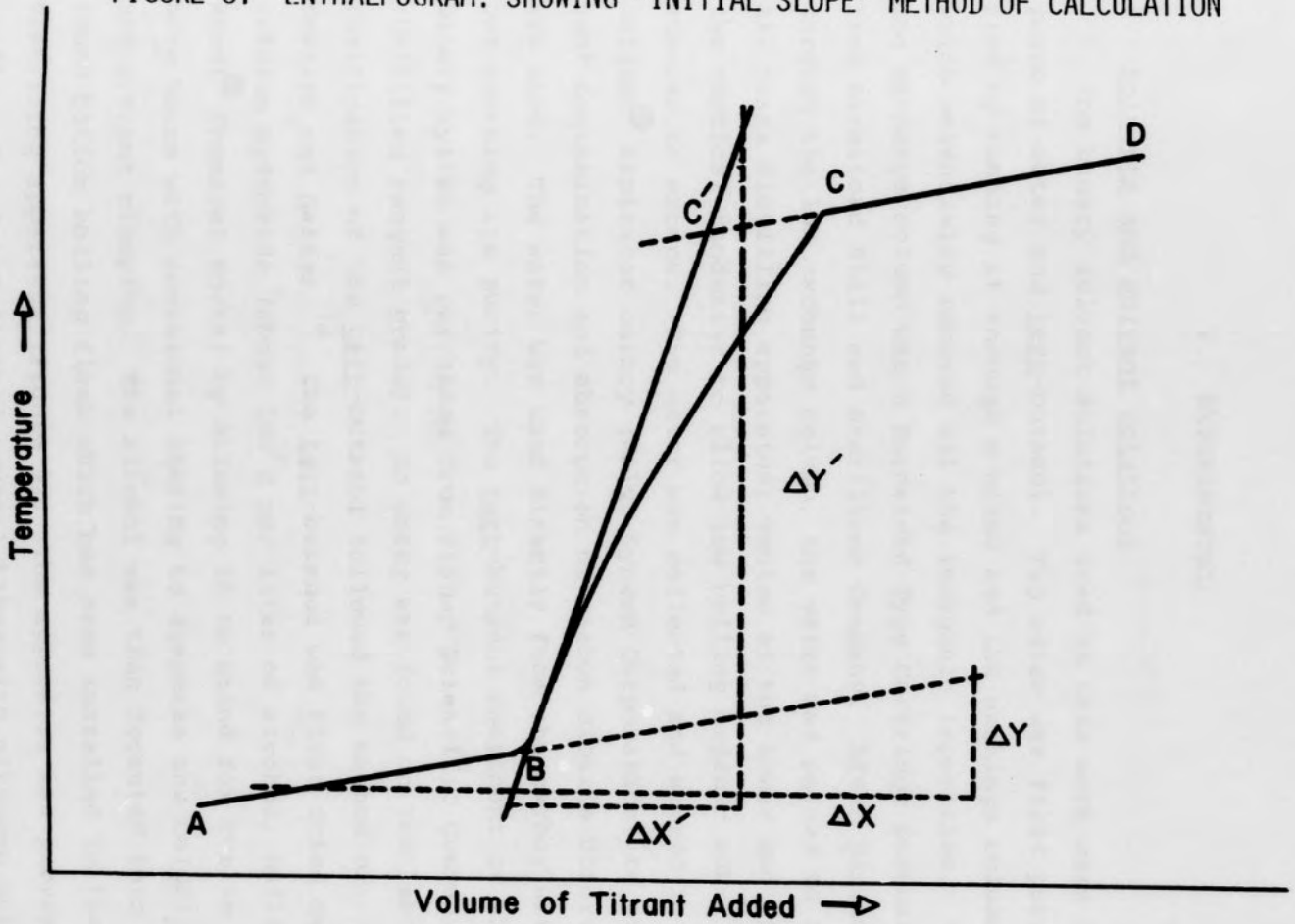

V. EXPERIMENTAL

A. Solvents and Solvent Solutions

The binary solvent solutions used in this work were composed of water and tert-butanol. Tap water was first purified by running it through a mixed bed ion exchange column which essentially removed all the inorganic impurities. The ion exchange column was a Barnstead Type Cartridge purchased from Barnstead Still and Sterilizer Company. After passing through the ion exchange column, the water was passed to an all glass distilling apparatus, vented at the lower end of the vertical condenser to allow low boiling organic substances to escape. The water was collected and stored in a Nalgene® aspirator carboy (Nalge Sybron Corporation) to prevent contamination and absorption of carbon dioxide before it was used. The water was used directly from the carboy without checking its purity. The tert-butanol component of the binary system was purchased from Fisher Scientific Company (Certified reagent grade). No assay was found on the label. Purification of the tert-butanol followed the method of DeVries and Saffer.[74] The tert-butanol was first dried over calcium hydroxide (about 100 g per liter of alcohol, Mallinckrodt® Chemical Works) by allowing it to stand for twelve or more hours with occasional shaking to disperse the $Ca(OH)_2$ and prevent clumping. The alcohol was then decanted into a round bottom boiling flask which had been installed in the distilling apparatus (Figure 9). The apparatus was previously flame dried and flushed several times with nitrogen which

FIGURE 9. DISTILLATION APPARATUS

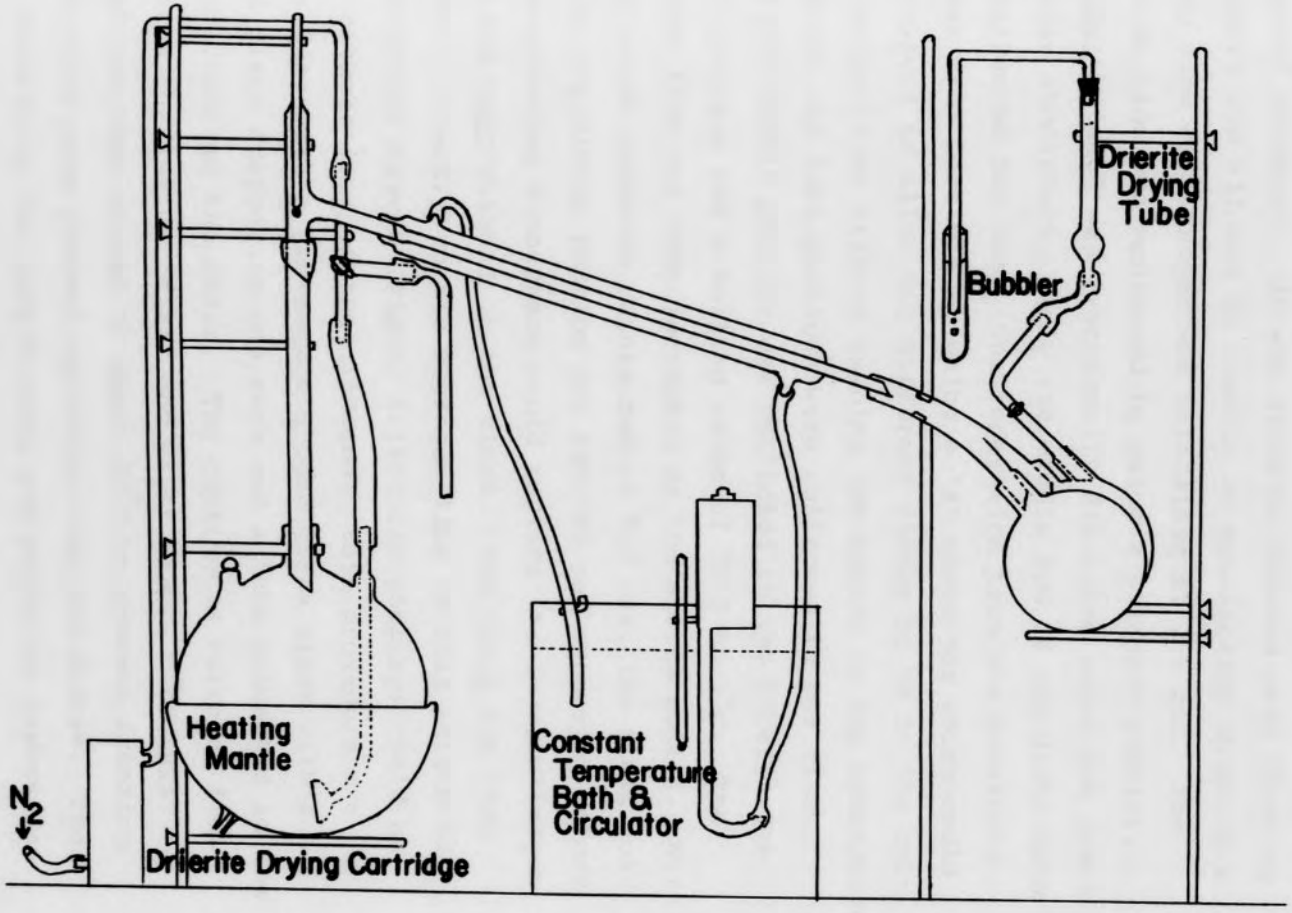

had been passed through indicating Drierite® (W. A. Hammond Drierite® Company). It was evacated between each flushing procedure and allowed to come to an equilibrium in which a steady flow of nitrogen was maintained at 2.5 psi. The nitrogen flow was monitored by using a standard bubbler. The tert-butanol was fractionally distilled under the inert nitrogen atmosphere. Only the middle 80% of the distillate was collected for use. The separation from the remaining 20% was made possible by using a "Y" connector which could be revolved to allow two different flasks to be in the collecting position without opening the system to the atmosphere. The first and last portions were collected in one flask, while the middle portion was collected in the other. The middle portion had a boiling range of 79.5-80.5°C. The nitrogen flow was then increased as the system cooled. With the nitrogen pressure maintained at 5-7 psi, the flask containing the middle portion was removed and stoppered before the surrounding atmosphere could replace the inert nitrogen above the tert-butanol in the flask. The flask was then connected directly to the nitrogen line so that activated 4 Å molecular sieves (Fisher Scientific Company) could be added without loss of the nitrogen. This procedure was easily done with a two-necked ground glass flask with a ground glass stopper in one neck and a tube connected to the nitrogen tank in the other. The continuous nitrogen flow minimized the influx of air and water vapor. The tert-butanol was then stored at about 30°C to prevent freezing and to allow some thermal agitation over the sieves. The flask containing the tert-butanol and molecular sieves was also shaken occasionally to facilitate better drying. The

water content was checked *via* Karl Fischer titration using a Junior Aquatrator made by Precision Scientific Company. The Karl Fischer reagent (Fisher Scientific Company) was first standardized by titrating a standard methanol-water solution. Four aliquots of distilled water of varying sizes were used to calculate the titer for the Karl Fischer reagent. A value of 0.9318 ± 0.0347 mg/ml was obtained. Four different samples of *tert*-butanol, in various stages of purification, were analyzed for water. The four samples taken were *tert*-butanol directly from the reagent bottle, freshly distilled but not stored under a nitrogen atmosphere, freshly distilled stored under a nitrogen atmosphere, and freshly distilled stored under nitrogen and molecular sieves. The data obtained is given in Table 1.

The results in Table 1 show that when the alcohol is distilled but not stored under nitrogen, the alcohol absorbs a significant amount of water. Also, distilling the alcohol and storing it under nitrogen is not sufficient because the results in column 3 show that under these conditions the alcohol still absorbs water as compared to the sample taken directly from the reagent bottle. However, when the alcohol is distilled and stored under nitrogen and molecular sieves for two weeks, the water content is reduced compared to that taken directly from the reagent bottle. Thus this purification method (distillation of alcohol, storage under nitrogen and molecular sieves) was the most efficient in the reduction of water content of the alcohol and was followed throughout the investigation. The slight but steady increase in the percentage water in the *tert*-butanol noted in the table can be explained as resulting

TABLE 1

Percentage of H_2O in tert-Butanol

Directly from Reagent Bottle

Sample #	% H_2O
1	0.0329
2	0.0301
3	0.0283
4	0.0299
5	0.0315
6	0.0296

Ave.=0.0305 ± 0.0013

Distilled, no Nitrogen

Sample #	% H_2O
1	0.185
2	0.244
3	0.178
4	0.223
5	0.175
6	0.197

Ave.=0.200 ± 0.022

Distilled with Nitrogen

Sample #	% H_2O
1	0.0897
2	0.0924
3	0.0921
4	0.0938

Ave.=0.092 ± 0.0116

Distilled, N , sieves

Sample #	% H_2O
1	0.00478
2	0.0107
3	0.0208
4	0.0270
5	0.0297
6	0.0372
7	0.0372

Ave.=0.0239 ± 0.0102

from a steady influx of water vapor caused by opening the flask over a four hour period to remove the seven aliquots for analysis. However, this problem was eliminated in actual use of the alcohol because the method used to remove it prevented water vapor from entering the flask. It would seem, then, that the alcohol was much drier than indicated by the average figures given in the table.

The water--alcohol binary systems were prepared in the following manner. First, cleaned and air dried bottles were weighed to the nearest tenth of a gram. The required amount of distilled water was added and the bottle containing the water was reweighed. The weight of the water was calculated by difference and reported to the nearest tenth of a gram. Next, the tert-butanol was added by using a 50 ml syringe (Fisherbrand, Fisher Scientific Company). The syringe was pushed manually through the septum into the reagent bottle containing the tert-butanol. Nitrogen pressure above the tert-butanol was used to push the alcohol into the syringe. Nitrogen pressure was selected to fill the syringe over manual manipulation to prevent a vacuum from forming in the storage flask as tert-butanol was removed. This procedure minimized the amount of moist atmosphere entering the storage flask. Before completely withdrawing the needle from the storage flask, a small volume of nitrogen was trapped in the tip of the needle. This nitrogen trap prevented any direct contact between the moist atmosphere and the tert-butanol in the transfer from the storage flask to the bottle containing the water. Thus, the alcohol that was transferred to the bottle contained no significant amount of water and the percentage of water in the binary

system was calculated based only on the specified amount of water added to the system. The solvent composition was computed in terms of mole percent alcohol.

$$\text{Mole \%} = \frac{\text{Moles}_{\underline{\text{tert}}\text{-BuOH}} \times 100}{\text{Moles}_{\underline{\text{tert}}\text{-BuOH}} + \text{Moles}_{H_2O}} \qquad \text{Eq. 43}$$

B. Chemicals

Hydrochloric acid (ACS reagent grade, Fisher Scientific Company) was diluted to approximately 0.1 M with distilled water and used as a titrant for the NaOH, tris(hydroxymethyl)-aminomethane, and $AgNO_3$. The HCl was standardized in the usual manner by precipitation with a small excess of $AgNO_3$.

Tris(hydroxymethyl)-aminomethane, THAM, (Fisher Certified, ACS grade, 99.97%) was used as received as a titrand.

Sodium hydroxide (Fisher Certified, ACS grade, 50% w/w solution) was diluted to a millimolar concentration and used as a titrand.

Silver nitrate (Certified ACS grade, Mallinckrodt® Chemical Works) was used as received as a titrand at about 0.1 M.

Sodium iodide (Fisher Certified reagent) was used as received as a titrand.

Silver perchlorate (anhydrous, G. Frederick Smith Chemical Company) was stored in a desiccator charged with Drierite®. The thermometric titrant solutions were standardized via the usual gravimetric procedure using a slight excess of sodium chloride (Fisher Scientific Company) solution.

Stock solutions of sodium tetraphenylborate, NaTPB, (Fisher Certified, ACS grade, 99.9%) were not prepared because of possible decomposition. Only the required amount of 50 ml was made and used immediately. The titrand was

prepared by pipetting 50 ml of the solvent or solvent mixture into the sample cell and adding the desired amount of NaTPB directly. The volume increase was assumed to be negligible. The solid NaTPB reagent was stored in a desiccator charged with Drierite®.

The tetraphenylarsonium chloride-hydrochloride (Eastman Organic Chemicals, Distillation Products Industries) was converted to tetraphenylarsonium chloride, TPAsCl, before use as a titrant following a modification of the method of W. T. Bolleter and R. J. Baczuk.[77] Their basic idea was followed, but due to lack of details the procedure had to be developed independently. The TPAsCl-HCl was converted to TPAsOH by an ion exchange technique on a column (1.0 in diameter x 30 in long) packed with strong base organic anion exchanger {Rexyn 201($Cl-SO_4$) polystyrene alkyl quaternary amine, in the Cl^- and $SO_4^=$ form, medium porosity, Fisher Scientific Company}. The resin was previously converted to the hydroxide cycle by running 3 liters of 25% w/w NaOH solution through the column. A glass plug was inserted at the bottom and top of the resin column to prevent the resin from passing through the column and floating when the NaOH was being run through. A $AgNO_3$ test was applied to the eluent to make sure all the Cl^- and $SO_4^=$ was removed. To prevent the TPAsCl-HCl from solidifying during the exchange the column was kept at 40-50°C with electric heating tape. Distilled water was used as the eluting solvent. Approximately 500 ml of distilled water was required to remove the TPAsOH from the column. Only the middle portion, about 300 ml, of the eluent collected was used because tests showed the bulk of the TPAsOH to be present in this portion. The

test used to determine the presence or absence of TPAsOH was to add 1 ml of $HClO_4$ to 2 or 3 drops of eluent. If TPAsOH were present it would precipitate as white $TPAsClO_4$. The supernatant liquid which was decanted after centrifuging was tested for the presence of Cl^- to be sure conversion was complete. A direct test on the eluent before removal of the $TPAs^+$ was not possible because the $TPAs^+$ ion is precipitated by NO_3^-. $TPAsNO_3$ is a white precipitate which cannot be distinguished from the white AgCl which might precipitate. A positive test for the Cl^- was never obtained while the TPAsOH was being collected. The TPAsOH solution was then reconverted to TPAsCl by neutralization with HCl. A digital pH meter (Model EU-200-30, Health-Schlumberger) was used to follow the neutralization process to a pH of 7.00. The reactions are:

$$TPAsOH + HCl \longrightarrow TPAsCl + H_2O \qquad \text{Eq. 44}$$

$$NaOH + HCl \longrightarrow NaCl + H_2O \qquad \text{Eq. 45}$$

The solution of TPAsCl and NaCl was evaporated to 40-50 ml and the TPAsCl crystallized out. It was expected that only TPAsCl would crystallize out because the solubility of NaCl is about four times greater than the solubility of TPAsCl, 35.7 g/100 ml[78] to 9.75 g/100 ml[73] of water at 25°C. Also the solubility of TPAsCl was decreased by the presence of NaCl in the solution. The TPAsCl crystals were dried in a desiccator. Faithful and Wallwork have shown that one formula unit of crystalline salt contains two water molecules.[79] The melting point range of the recrystallized $TPAsCl \cdot 2H_2O$ was 254-257°C as compared to 258-260°C reported in the Merck Index.[80] Since the melting point range was in good agreement with the value found in Merck Index, no further purification

was done. The approximate recovery after the ion exchange procedure was 81%. The $TPAsCl \cdot 2H_2O$ was subsequently used as a thermometric titrant. The solutions were made by weighing the required amount of solid reagent and dissolving it in about 30 ml of distilled water or tert-butanol solvent mixture to yield a solution about 0.2 M. The titrant solution was standardized via the usual gravimetric procedure by precipitating with an excess of $HCl)_4$, filtering, washing with distilled water saturated with $TPAsClO_4$, and drying at 110°C.

C. Apparatus

The differential thermometric titration apparatus used in this investigation was similar to the one reported by Tyson, McCurdy, and Bricker.[62] Extraneous heats, such as heats of dilution and stirring, are significantly minimized in the differential apparatus since the two cells of a differential system are exposed to an identical environment and identical conditions except for the reaction in the sample cell.

The apparatus can be divided into two sub-divisions consisting of the mechanical parts and the electrical circuitry. The mechanical parts consisted of the structural framework, titrant delivery system, and the stirring mechanism. The electrical components consisted of the calibration heater and temperature sensing systems. The mechanical components of the instrument are best described using diagrams of the instrumentation (Figures 10, 11, and 12).[81] The frame was constructed from solid aluminum flexaframe rods and was connected at the corners with flexaframe hook connectors purchased from Fisher Scientific Company. The flexaframe construction was approximately 4 ft long, 2 ft high,

FIGURE 10. THERMOMETRIC TITRATION APPARATUS

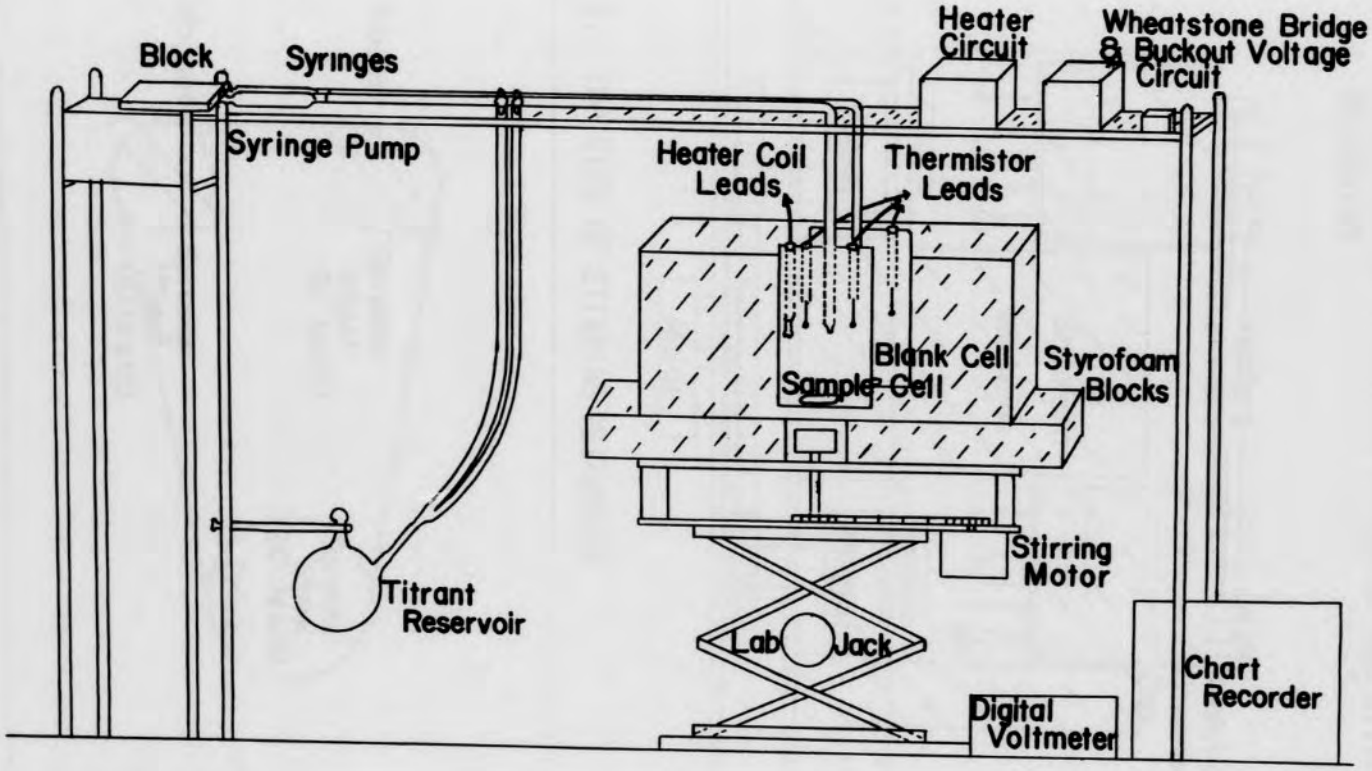

FIGURE 11. SIDE VIEW OF TITRATION APPARATUS AND STIRRING MECHANISM

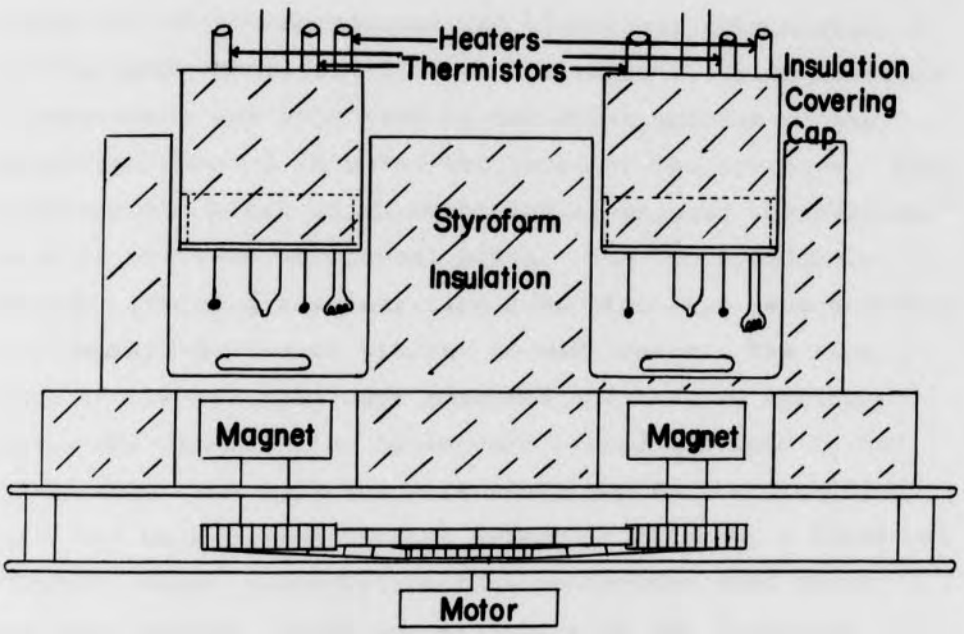

FIGURE 12. TOP VIEW OF STIRRING MECHANISM

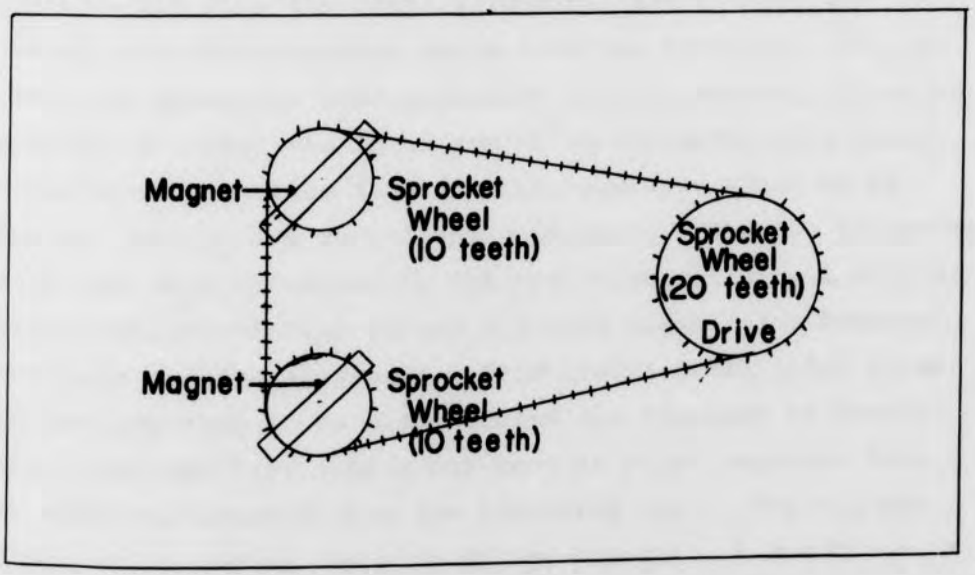

and 15 in wide. The top of the structural framework was covered with 1/8 in thick hardboard which supported essentially all of the mechanical and electrical components. A syringe pump (Model 234-2, Sage Instruments, Orion Research Incorporated) was supported by two cross members of the flexaframe about 3 in below the level of the syringes. This permitted the block which mechanically engaged the syringes to be in the same horizontal plane. The two hypodermic syringes (Yale, glass luer tip, 2 ml capacity, Becton-Dickinson Company) delivered titrant to both cells. The flow rates of six syringes were measured and the two syringes having the closest flow rates were paired and used in the instrument. The syringes were connected to the titration cells and to a common titrant reservoir flask by a three-way stopcock, short polyethylene tube connectors, and glass capillary tubing. With one alignment of the three-way stopcocks, titrant was drawn from the titrant flask into the syringes and with the other alignment, the titrant was injected into the titration cells from the syringes. The two three-way stopcocks were connected to the reservoir flask by a glass "Y" tube, the lower arm being connected to a ground glass connecting tube to allow the reservoir flask to be removed for filling and cleaning purposes. The two three-way stopcocks were connected to the titration cells by 1 mm i.d. glass capillary tubing having a ground glass joint between the cells and the stopcocks. This ground glass joint allowed the apparatus to be disassembled for cleaning or repairing. The capillary tubing was bent at a 90^{o} angle so that it could be inserted into the titration cell. The tip was drawn out to reduce the size of the opening. A reduction in

the size of the capillary buret tip was required to prevent premixing of the titrant and titrand solutions (Figure 13). The two titration cells were made from polyethylene, 90 ml capacity, screw-cap containers (Figures 11 and 13). Six holes were drilled in each cap. They housed two baffle plates positioned directly in front of the thermistors, the 6 mm o.d. glass tubing sections approximately 10 cm in length through which two thermistors and a heating coil were inserted, and a hole in the center for the buret tip. The baffle plates were needed to dissipate the vortex caused by stirring. If a vortex formed, it would expose the thermistors to the atmosphere above the solution in the cells. The buret tip, the three glass tubing sections, and the two baffle plates were secured to the cap with epoxy. The thermistors and heating units were secured to the glass tubing sections with silicone rubber cement (G.E., RTV108, Translucent Silicone Rubber Adhesive). The silicone rubber adhesive was used because it was waterproof and easily removed if the thermistors had to be changed. The two cells were placed in a large block of styrofoam, hollowed out to the exact size of the polyethylene caps. A portion of the removed styrofoam was used to cover the cap as shown in Figure 11. The bottom or main block could be removed very easily when the support, a lab-jack (medium, Fisher Scientific Company) supporting the stirring mechanism, was lowered. This was necessary for easy access to the titration cells. The stirring mechanism was composed of a wooden frame, which housed a synchronous motor (Model GA, 300 rpm, Hurst Synchronous Motor Company). The motor was used to turn two ceramic, 1 in x 1 1/2 in x 1/4 in bar magnets (Edmund

FIGURE 13. CUTAWAY VIEW OF SAMPLE AND BLANK TITRATION CELLS

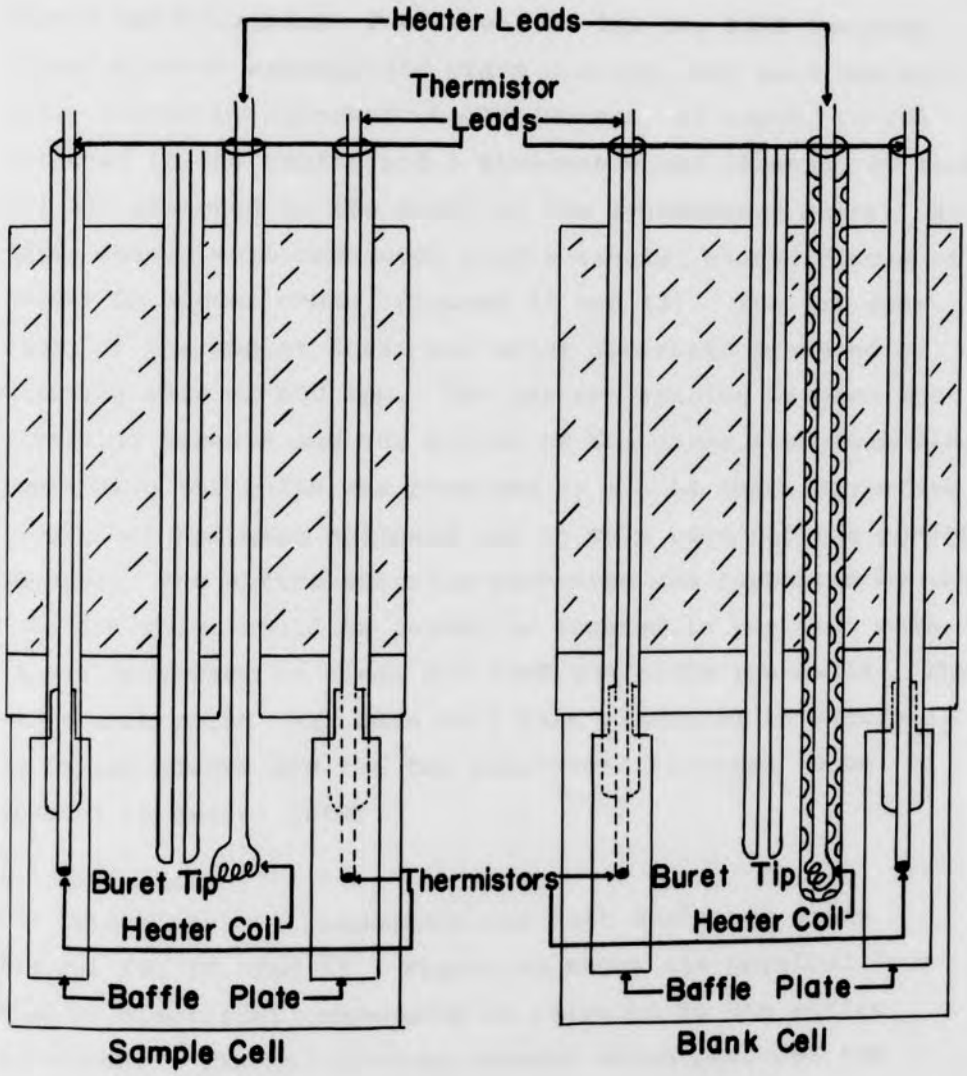

Scientific Company) which drove the Teflon® covered bar magnet inside the titration cells (Figure 11). The two revolving magnets under the titration cells were epoxied to two 3 in steel shafts, 5/16 in diameter, held in position by Boston Self-Aligning, Precision, XL-1/2 in, Ball Bearings fitted with an appropriate brass bushing, and were mechanically turned by sprocket wheels (Boston, 10 teeth, C1-10) attached to the shafts and a sprocket wheel (Boston, 20 teeth, CB1-20) attached to the shaft of the synchronous motor. All three wheels were connected with a single, closed circle of Number 1A ladder chain (Figures 11 and 12). The 1:2 gear ratio of the magnet shaft and motor sprockets produced a stirring rate of 600 rpm. The correct spacing between the revolving magnets and the bottom of the large styrofoam block containing the cells was provided by a 2 in thick styrofoam block that had been hollowed out to make room for the ceramic magnets. The entire stirring mechanism was supported by the lab-jack which could be raised or lowered in position when it was necessary to clean and load the titration cells. The other main parts that have only been simulated in Figure 10 as square blocks are the two electrical circuits to be covered in detail later.

D. Circuitry

The elctrical components are best described using Figures 10, 14, and 15. Figure 10 shows the physical location of electrical components in relation to the entire instrument. The calibration circuit which produces the electrical heating in either cell and the sensing circuit which measures the temperature change in the sample cell are diagrammed in Figures 14 and 15 respectively. The

FIGURE 14. CALIBRATION HEATING CIRCUIT

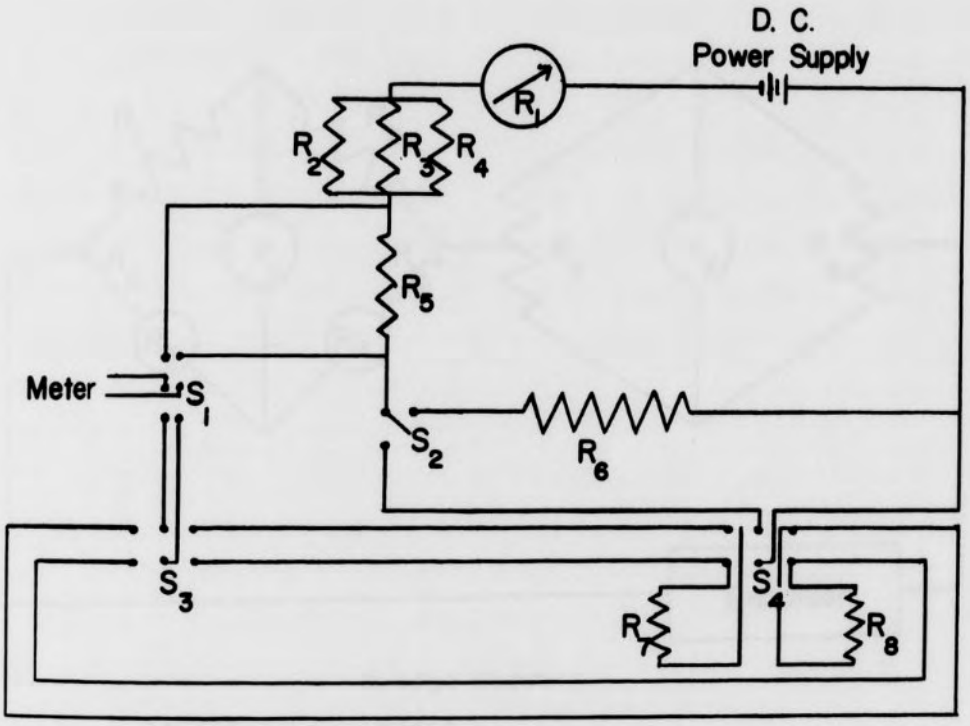

R_1 = current control

R_2 = R_3 = R_4 = 60 ohm resistors

R_5 = 1 ohm, standard resistor

R_6 = 10 ohms, dummy resistor

R_7 = heating coil in blank cell

R_8 = heating coil in sample cell

S_1 = S_2 = S_3 = S_4 = Switches

FIGURE 15. TEMPERATURE SENSING AND BUCKING VOLTAGE CIRCUITS

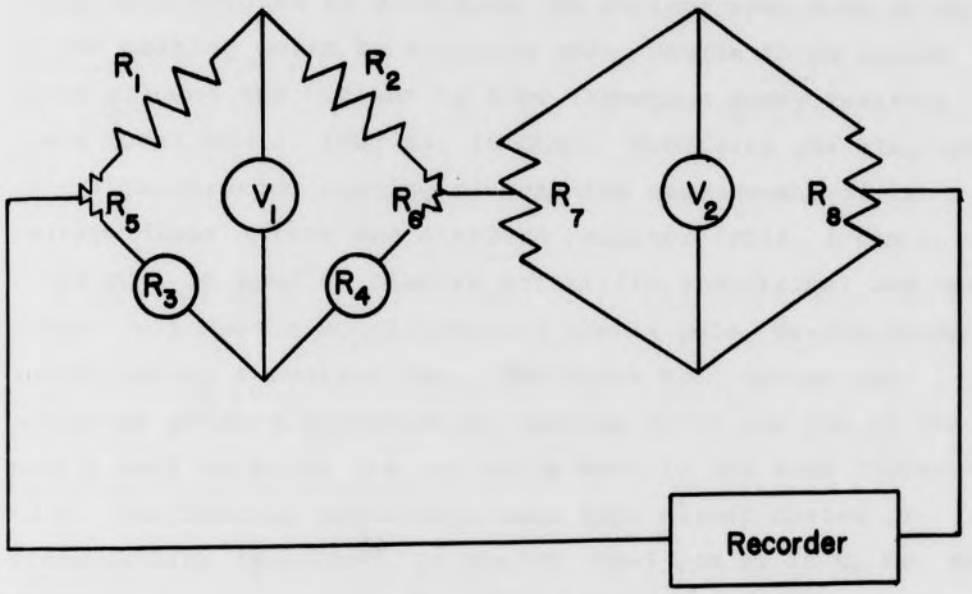

Bridge Circuit

$R_1 = R_2$ = 15 kilohm resistors

$R_3 = R_4$ = thermistor piles (15 kilohm)

$R_5 = R_6$ = 10 kilohm, 10 turn potentiometers

U_1 = two Mallory-Duracell Mercury Batteries (1.44 volts ea)

Buckout Circuit

R_7 = 10 kilohm, 1 turn potentiometer

R_8 = 500 ohm, 1 turn potentiometer

U_2 = one Burgess-42, Mercury Activator (1.4 volts)

calibration heating circuit supplied current to the sample or blank heater coils. The circuit (Figure 14) was electrically equilibrated by diverting the current away from either of the heating coils by a single pole, double throw switch which allowed the current to flow through a dummy resistor (Dale Model RH-10, 10w7044, 10 ohm). Provision was also made in the calibration heating circuit for measurement of the voltage drops across the standard resistor (RC4R, 1 ohm ± 0.01% TC ± 15 ppm/^{o}C, Electro Scientific Industries) and the sample cell heater by switching a double pole, double throw switch during a heating run. The blank cell heater was activated after a titration or heating curve was run in the sample cell to bring the two cells back to the same temperature. The heating coils were made from enamel-coated resistance wire (Evanohm®, 83 ohm/ft, TC-5 ppm at 25^{o}C, No. 40, Precision Alloys, Wilber B. Driver Company). Approximately 1.5 in of the wire was also used to make each heater. The enamel was removed from both ends and soldered to two leads (Number 20 A.W.G., solid hook-up wire). The joints and exposed wire were covered with epoxy. The enamel and epoxy coating prevented the wire or solder from being exposed to the chemicals in the cells. The leads were connected to a double pole, double throw switch which controlled the current supplied to the individual cells. The resistances of the heating coils were approximately 12 ohm. The power source for the heating circuit was a Kepco D. C. Power Supply (Model PAT 15-1.5R, Kepco Incorporated). Located between the power supply and the two heating coils was a variable potentiometer current control (Model 21513, 30K, Amphenol Controls Division). This controlled the amount of current delivered

by the calibration circuit to produce heating curves of the desired slope.

A Wheatstone bridge, containing the temperature-sensing devices (Figure 14), was used to monitor the temperature difference of the cells. Two legs of the Wheatstone bridge had 15 kilohm resistors (Model 7027, TWR Incorporated) plus 5 kilohm from the corner potentiometer (set halfway, Type 8400, 10K ohm, TRW Incorporated) which resulted in a total of 20 kilohm for each arm. The two other legs were composed of a pair of thermistors connected in parallel having a resistance of approximately 15 kilohm at 25°C (paired to average any heat gradients of improper mixing). The thermistor leads were soldered to a shielded cable about 12 in long. The other end of the cable was soldered to a connector in the heating circuit chassis box and grounded. The bridge circuit was powered by two Mallory-Duracell Mercury Batteries, 1.44 volts each, connected in series. The buckout unit was used to balance the system and zero the chart recorder. The course adjustment was a 10 kilohm potentiometer (TWR Incorporated, Model SD103 A) and the fine adjustment was a ten-turn 500 ohm potentiometer (Model 532, Spectrol). The buckout was powered by a single Burgess Hg-42, Mercury Activator, 1.4 volts. These circuits were contained in aluminum chassis boxes, 4 in x 6 in x 4 in. The internal connecting wire used in assembling the circuits was Number 20 A.W.G. hook-up wire. The leads (2 conductor, braided shield, plastic jacketed, miniature microphone cable, Belden) to the recorder and the thermistors were all grounded. All other power lines, leads, recorder, metal containers, and power supplies were grounded to reduce noise from inside or outside the system. A Weston

Model 1240 Digital Multimeter (Weston Instrument Division) was used to measure the voltage drop across the heater and the standard resistor and a millivolt recorder (Speedomax XL, low profile--600 series, Leeds and Northrup) was used to record the titration curves.

E. Testing and Calibration

1. Thermistor Resistance

Thermistors (30 kilohm ± 20% at 25°C, T.C. of R. -4.5%/degree, Dissipation Constant in distilled H_2O 5 MW/°C, Type A43R, Victory Engineering), the temperature sensing elements of this system, are metal oxide semi-conductors. Their resistance is inversely proportional to temperature change, $\Delta R / \Delta T$, and is not linear except over very small temperature ranges (Figure 16).[64] The thermistors in this system made up two arms of the Wheatstone bridge. It is imperative that the two adjacent arms of the Wheatstone bridge be closely matched, otherwise the arms would not respond to the same degree to identical temperature changes. Two dozen thermistors were tested at 25°C to obtain two pairs whose parallel resistances matched closely. The results of the testing are shown in Table 2.

TABLE 2
Thermistor Resistances

Series		Parallel	
Thermistor No.	Resistance (kilohm)	Thermistor Nos.	Parallel Resistance
2	28.78	2 & 18	14.33
3	28.55		
18	28.53	3 & 20	14.21
20	28.30		

FIGURE 16. RESISTANCE AS A FUNCTION OF TEMPERATURE FOR THERMISTORS AND METALLIC CONDUCTORS

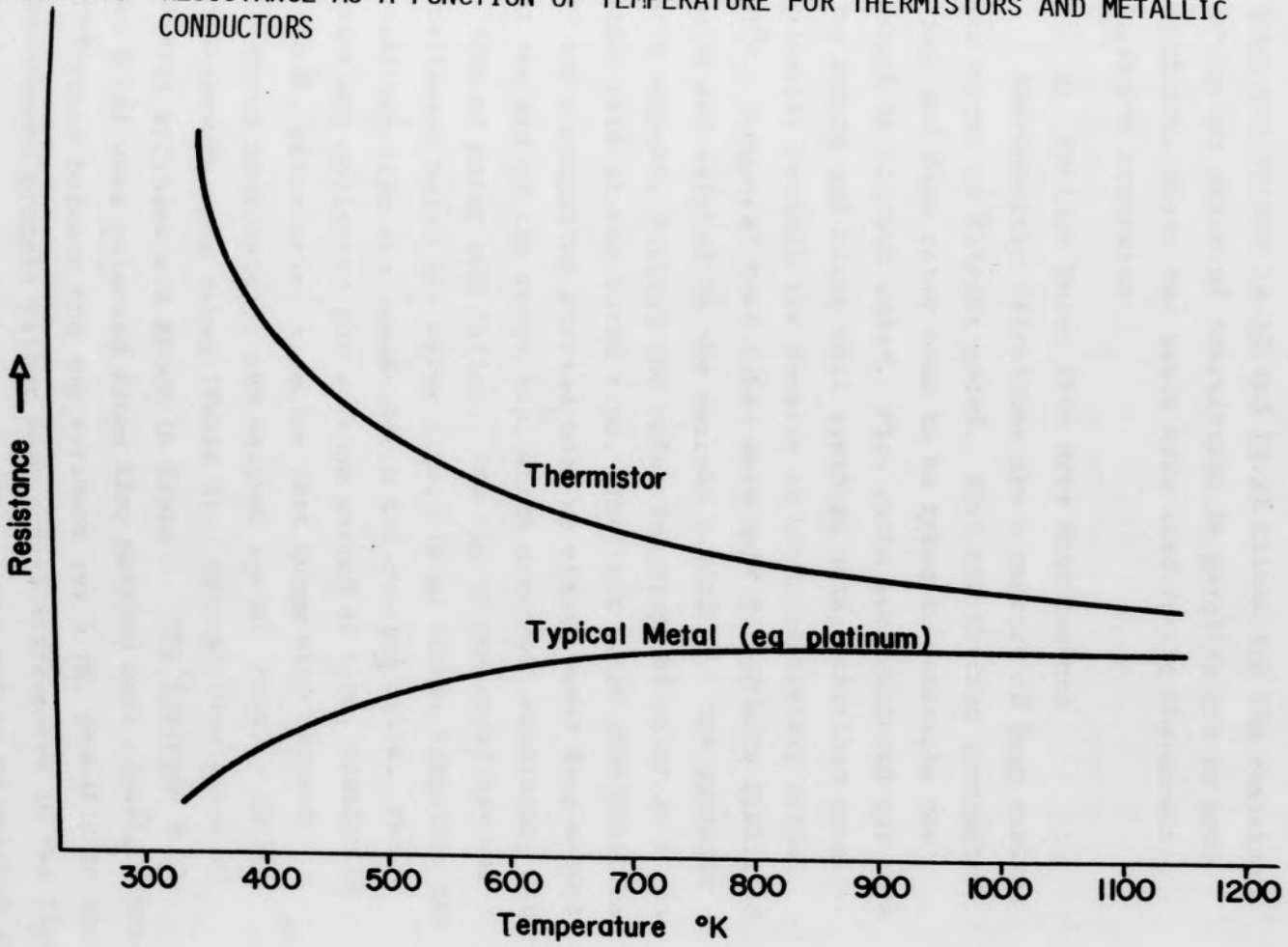

Since the values 14.33 and 14.21 kilohm for the resistance of the two pairs of thermistors in parallel are in good agreement, these two pairs were used in the thermometric titration apparatus.

2. Syringe Buret Flow Rate Measurements

Thermometric titrations are a measure of heat evolved per volume of titrant added. Both the titrant (concentration) and flow rates need to be known to determine the amount of titrant added. Flow rates were measured for both the sample and blank cell syringes using distilled water, primarily because its density is known accurately around 25°C. Stoppered test tubes were half filled with distilled water and weighed to the nearest 0.00001 g. The syringes were engaged, forming and releasing drops of water at a constant rate at the buret tips. The test tubes were positioned and a stopwatch started when no visual water drop showed at the end of the buret tip, which occurred immediately after a drop of water had fallen. The tip of the capillary was positioned below the water line. In an actual titration the capillary tips are submerged in the charged cells. The water was collected for a known period of time, usually 60 seconds, after which time the test tubes were removed, stoppered immediately, and weighed again. Usually 10-12 measurements were taken (Table 3). Typical flow rates of several syringes are shown in Table 4. The syringes B 372 and B 083 were selected since they matched most closely. The difference between the two syringes was 0.3%, probably in the measurement process rather than actual differences in the flow rate of the two syringes. The flow rates had to be matched so that heats of dilution would cancel each other between the

TABLE 3

Flow Rate of Syringes Used (ml/sec)

Syringe No. B373	Syringe No. B083
0.01053	0.01052
0.01047	0.01058
0.01052	0.01054
0.01057	0.01054
0.01061	0.01060
0.01041	0.01053
0.01051	0.01052
0.01055	0.01061
0.01052	0.01056
0.01060	0.01062
0.01054	0.01054
Avg. = 0.01053 ml/sec	Avg. = 0.01056 ml/sec

TABLE 4

Flow Rates of Six 2 ml Syringes Tested

Syringe No.	Flow Rate (ml/sec)
B372	0.01053 ± 0.00004
B417	0.01044 ± 0.00005
B029	0.01060 ± 0.00003
B083	0.01056 ± 0.00003
B080	0.01047 ± 0.00011
B955	0.01017 ± 0.00017

two cells in the differential thermometric titrations.

3. Titration Procedure

The procedure followed in doing thermometric titrations can be subdivided into five steps. The first step was filling the syringe burets. The titrant reservoir had to contain a minimum of 30 ml. The syringes were filled by aligning the three-way stopcock correctly and manually pulling back on the syringe plunger. Provision was made using the two-neck reservoir flask for filling the syringes with N_2 pressure if air sensitive or hydroscopic nonaqueous solvents are to be used. All air bubbles were removed by forcing them out through the buret tips. When the syringes and lines were filled with titrant and all bubbles removed, the plungers were drawn back slightly to form small air spaces at the buret tips. This prevents the premixing of titrant and titrand when the cells are positioned and allows for thermal expansion of titrant solution. The two cells were then filled with 50 ml of the appropriate solution. The second step, the most time consuming, was obtaining a nearly isothermal condition between the two cells. The temperature differential of the system was checked by watching the drift of the chart recorder. If the drift was small or absent it was assumed that the system was nearly isothermal. When the pen drifted a great deal, this indicated that the two cells were not at the same temperature, the direction of the drift indicating which cell was cooling at the faster rate. When this had been determined, the temperature of the other cell was raised by warming with the hand or by using an internal heater. This procedure was continued until the drift was acceptable. Then the large block of styrofoam was positioned

around the two cells. A base line was run for at least 30 sec to again check that an isothermal condition existed. However, it was impossible to prevent all drift and thus a base line correction was made in the calculations. After the base line was drawn, the titration was started by activating the syringe pump. A generalized titration curve (Figure 8) shows the three sections as they appear in an actual enthalpogram: a pretitration base line, AB, actual titration curve, BC, the extrapolated initial slope line, BC', and a posttitration line, CD. When the reaction was completed, the pen would show about the same drift for both the pretitration line, AB, and the posttitration line, CD. Any differences in the base line slope, AB, and the excess titrant slope, CD, was caused by differences in temperature of titrant and titrand and/or the increase in the cooling rate of the heated cell. When the excess titrant line, CD, appeared, the titrant was stopped. The blank cell was heated to the same extent as the sample cell had been by the reaction. This was monitored by heating the blank cell until the recorder pen returned to the original base line position. The system was calibrated in the fourth step by running three heating curves. The procedure remained the same as that described for a titration except that the calibration heater in the sample cell caused the movement in the recorder, whereas the heat of the reaction caused the movement in the titration curve. Three heating curves were done to obtain an average for the calibration. In step five, the electrical systems were turned off or disconnected and the cells were removed and emptied. All components inside the cups and the cups themselves were washed with an appropriate solvent and distilled water from

squeeze bottles. The system was then rinsed with acetone which dried it faster than air drying. Having cleaned and dried the system, it was then ready for another run. About one hour was usually required to complete the five steps. As mentioned previously the raw curves from the chart recorder were interpreted by the 'initial slope' extrapolation method.[74] The 'initial slope' line and the base line, which served only as a correction for the 'initial slope' line, were drawn with a straight edge by sighting down the line and straight edge to make the alignment. The X and Y coordinates were measured to the nearest 0.01 cm for the base line AB and the titration line BC' (Figure 8). A simple computer program was used to do the calculations (Appendix). The equation solved by the computer was:

$$\Delta H = E_1 E_2 S_1 / 4.185\ RNFS_2 \qquad \text{Eq. 46}$$

The input data included voltages across the heating coil, E_1, the voltage across the standard resistor, E_2, the resistance of the standard resistor, R, in ohm, concentration of titrant, N, in mol/l, the flow rate, F in ml/sec, the X and Y coordinate changes of the titration, heating and base line in cm. The output consisted of the individual slopes of the heating curves and the titration curves corrected for base line drift, the average of the calibration heating slopes, the enthalpy values for each calibration entered, the average enthalpy value, deviations from the average, and the percentage deviation of the values. The program was designed to allow for fluctuations in the number of heating curves, statement 7, in the number of titrations per set, statement 4, and in the number of sets, statement 2. The printout of individual data for each set could be scanned quickly and any major errors

in measurement or in drawing of the slopes for the lines could be detected and eliminated. After the data was plotted more revealing information and interpretations were made. These interpretations will be developed in a later section.

4. Calibration Reactions

Three reactions of known enthalpy change were used to test and calibrate the system. The reactions were HCl-NaOH, HCl-THAM, and HCl-$AgNO_3$. Table 5 gives the results obtained.[62,81]

TABLE 5

Calibration Reactions

Reaction	Number of Runs	ΔH^{o}exp. (k.cal./mole)	ΔH^{o}(lit) (k.cal./mole)
HCl-NaOH	7	13.37 ± 0.27	13.36
HCl-THAM	9	11.58 ± 0.22	11.55
HCl-$AgNO_3$	10	15.52 ± 0.27	15.64

The experimental values for the enthalpies of the three reactions agreed well with the reported values. Thus, based on these results, the titration apparatus constructed seems to produce both reasonable accuracy and precision.

VI. RESULTS AND DISCUSSIONS

Various slightly soluble salt precipitation reaction probes have been investigated to determine their usefulness in the study of water structure changes. Data has been obtained for three probe reactions. These reactions are:

$$AgClO_4 + NaI \longrightarrow NaClO_4 + \underline{AgI} \qquad \text{Eq. 47}$$

$$AgClO_4 + NaTPB \longrightarrow NaClO_4 + \underline{AgTPB} \qquad \text{Eq. 48}$$

$$TPAsCl + NaTPB \longrightarrow NaCl + \underline{TPAsTPB} \qquad \text{Eq. 49}$$

The data obtained for the above reactions are listed in Tables 6, 7, 8, 9, 10, and 11. There are two data tables for each reaction. The average enthalpy values obtained by the elimination of titration and/or calibration heating curves showing erratic behavior appear in the Tables of adjusted data. The average enthalpy values using all the raw data appear in the Tables of nonadjusted data. The precision of the enthalpy values are listed for both the adjusted and raw data. The precision of the raw data was 1.22 to 27.5% (relative average deviation). The same data adjusted as previously explained was 0.55 to 1.78%. Figures 17, 18, and 19 have the adjusted and nonadjusted data superimposed, which shows that the adjusted values are not significantly different from the nonadjusted and that the same curve exists for both sets of points. Thus, only the adjusted data will be considered in following discussions. The accuracy of several calibration reactions has been noted in the Experimental Section, and we assume that comparable results were carried over to these probe reactions. This assumption was supported by carrying out the precipitation of AgI in pure

TABLE 6

Unadjusted Data for $AgClO_4$-NaI

No. of Samples	Solvent (tert-BuOH)	Average Enthalpy (kcal/mole)	Relative Avr Dev %
8	0	$28.4_9 \pm 0.93$	2.48
6	2.005	$28.2_9 \pm 0.42$	1.22
7	2.654	$28.1_5 \pm 0.83$	2.14
7	3.413	$27.6_0 \pm 1.21$	3.74
7	4.326	$28.3_6 \pm 1.19$	3.16
7	6.073	$28.2_5 \pm 0.54$	1.41
7	7.465	$26.0_5 \pm 0.65$	1.87
6	8.865	$24.2_2 \pm 1.94$	5.93
7	10.32	$26.1_2 \pm 0.63$	1.95
8	20.46	$24.8_8 \pm 0.54$	1.67
8	33.70	$23.3_2 \pm 0.55$	1.85
6	49.60	$22.3_5 \pm 0.63$	2.45
5	68.46	$21.0_3 \pm 0.71$	2.25
6	89.96	$19.5_2 \pm 0.57$	1.87
6	95.37	$20.9_4 \pm 1.03$	3.94

TABLE 7

Adjusted Data for $AgClO_4$-NaI

No. of Samples	Solvent (tert-BuOH)	Average Enthalpy (kcal/mole)	Relative Avr Dev %
5	0	$26.7_0 \pm 0.24$	0.69
6	2.005	$28.3_1 \pm 0.23$	0.65
6	2.654	$28.4_8 \pm 0.26$	0.74
5	3.413	$27.4_1 \pm 0.46$	1.20
5	4.326	$28.4_1 \pm 0.26$	0.72
6	6.073	$28.0_9 \pm 0.39$	0.97
7	7.456	$26.1_8 \pm 0.31$	0.84
5	8.865	$23.8_9 \pm 0.29$	0.84
6	10.32	$26.2_0 \pm 0.30$	0.91
6	20.46	$24.7_2 \pm 0.18$	0.64
8	33.70	$23.2_9 \pm 0.25$	0.77
6	49.60	$22.2_3 \pm 0.22$	0.74
5	68.46	$20.9_0 \pm 0.18$	0.64
6	89.96	$19.4_2 \pm 0.23$	0.89
5	95.37	$20.7_8 \pm 0.85$	0.85

TABLE 8

Unadjusted Data for $AgClO_4$-NaTPB

No. of Samples	Solvent (tert-BuOH)	Average Enthalpy (kcal/mole)	Relative Avr Dev %
8	0	$20.1_6 \pm 1.33$	3.88
7	2.005	$21.5_0 \pm 0.82$	2.86
6	2.654	$23.7_3 \pm 0.74$	2.52
6	3.413	$26.1_2 \pm 1.29$	3.53
7	4.326	$31.8_1 \pm 1.25$	3.23
7	6.073	$35.3_3 \pm 1.40$	2.59
6	7.465	$30.1_8 \pm 0.38$	1.00
7	10.32	$25.4_0 \pm 0.64$	1.95
6	20.46	$21.5_6 \pm 0.65$	1.97
7	33.70	$20.5_0 \pm 0.48$	1.94
6	49.60	$19.9_2 \pm 0.94$	3.14
6	68.46	$18.0_6 \pm 3.49$	3.49
6	89.96	$13.2_2 \pm 0.50$	2.70
6	95.37	$11.6_4 \pm 0.51$	4.22

TABLE 9

Adjusted Data for $AgClO_4$-NaTPB

No. of Samples	Solvent (tert-BuOH)	Average Enthalpy (kcal/mole)	Relative Avr Dev %
6	0	$20.1_6 \pm 0.24$	0.98
5	2.005	$21.5_0 \pm 0.35$	1.04
5	2.654	$23.4_6 \pm 0.35$	1.02
5	3.413	$26.3_5 \pm 0.27$	0.85
6	4.326	$31.7_3 \pm 0.42$	1.16
4	6.073	$34.9_8 \pm 0.20$	0.35
6	7.465	$30.0_5 \pm 0.22$	0.48
5	10.32	$25.5_0 \pm 0.30$	0.93
6	20.46	$21.4_4 \pm 0.27$	0.92
7	33.70	$20.2_7 \pm 0.20$	0.81
5	49.60	$19.8_0 \pm 0.15$	0.55
5	68.46	$18.1_5 \pm 0.17$	0.73
5	89.96	$13.1_0 \pm 0.14$	0.76
6	95.37	$11.4_5 \pm 0.14$	0.98

TABLE 10

Unadjusted Data for TPAsCl-NaTPB

No. of Samples	Solvent (tert-BuOH)	Average Enthalpy (kcal/mole)		Relative Avr Dev %
6	0	5.4_7	2.12	27.5
4	3.11	20.2_7	1.81	6.90
4	4.00	28.0_4	2.00	5.32
4	5.04	32.2_8	1.92	4.61
4	6.12	29.7_3	2.26	6.38

TABLE 11

Adjusted Data for TPAsCl-NaTPB

No. of Samples	Solvent (tert-BuOH)	Average Enthalpy (Kcal/mole)		Relative Avr Dev %
4	0	4.3_8	0.11	1.78
3	3.11	20.0_4	0.27	1.01
3	4.00	28.7_5	0.41	1.02
3	5.04	32.3_9	0.42	0.91
3	6.12	31.0_1	0.32	0.70

FIGURE 17. ENTHALPY OF REACTION FOR SILVER IODIDE PRECIPITATION ADJUSTED (△) AND NONADJUSTED (○) DATA IN TERT-BUTANOL--WATER MIXTURES

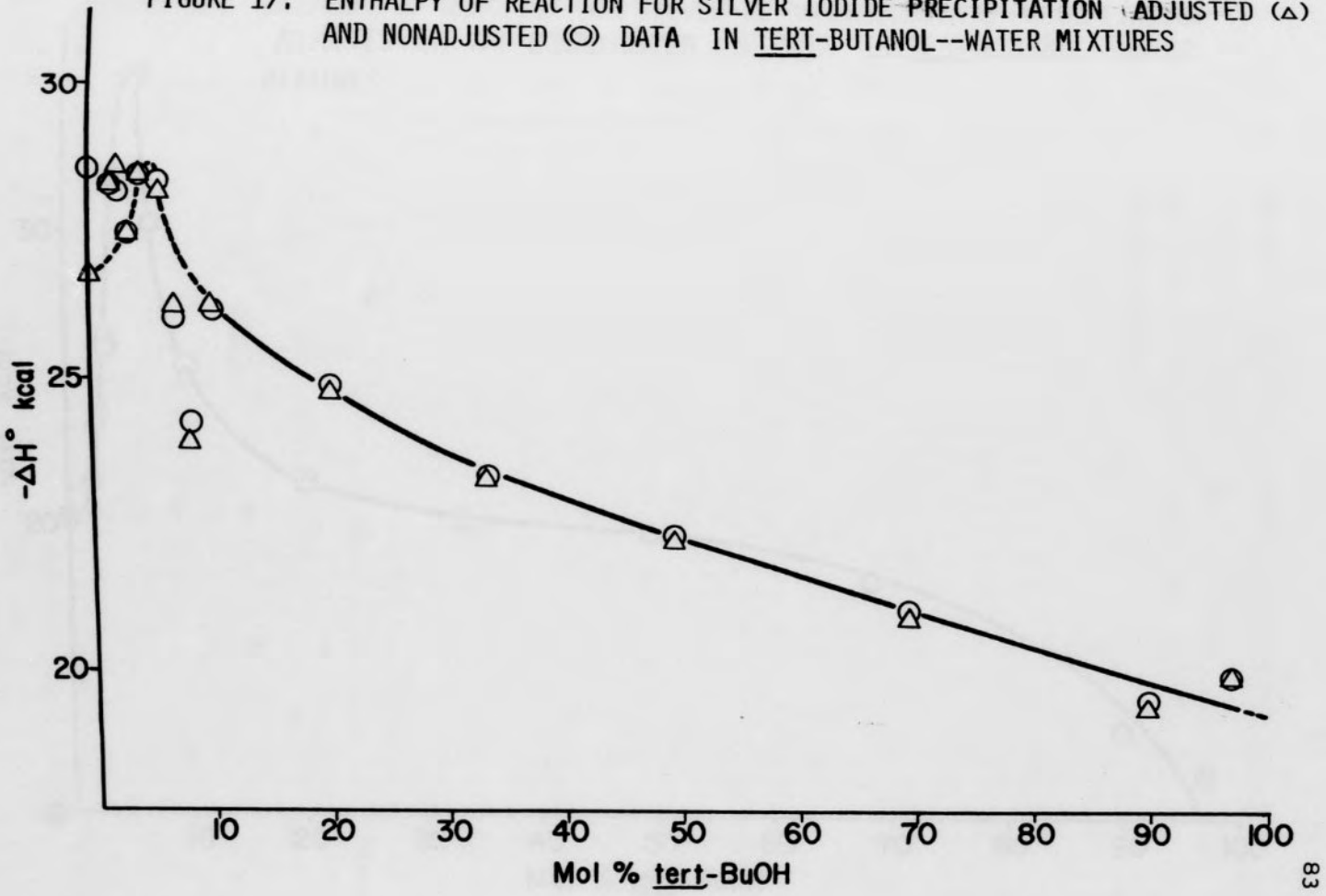

FIGURE 18. ENTHALPY OF REACTION FOR SILVER TETRAPHENYLBORATE PRECIPITATION ADJUSTED (△) AND NONADJUSTED (○) DATA IN TERT-BUTANOL--WATER MIXTURES

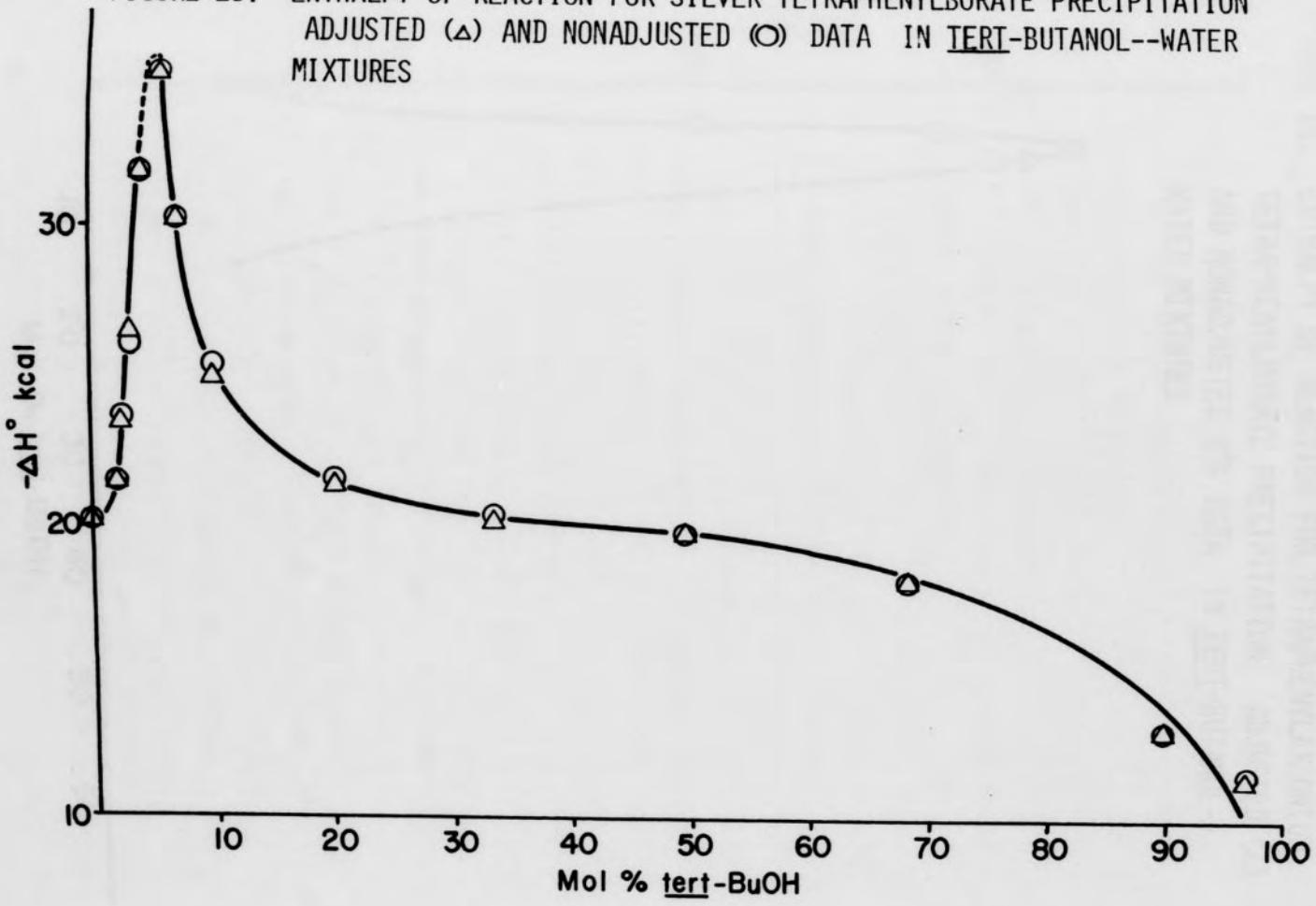

FIGURE 19. ENTHALPY OF REACTION FOR TETRAPHENYLARSONIUM TETRAPHENYLBORATE PRECIPITATION ADJUSTED (△) AND NONADJUSTED (○) DATA IN TERT-BUTANOL--WATER MIXTURES

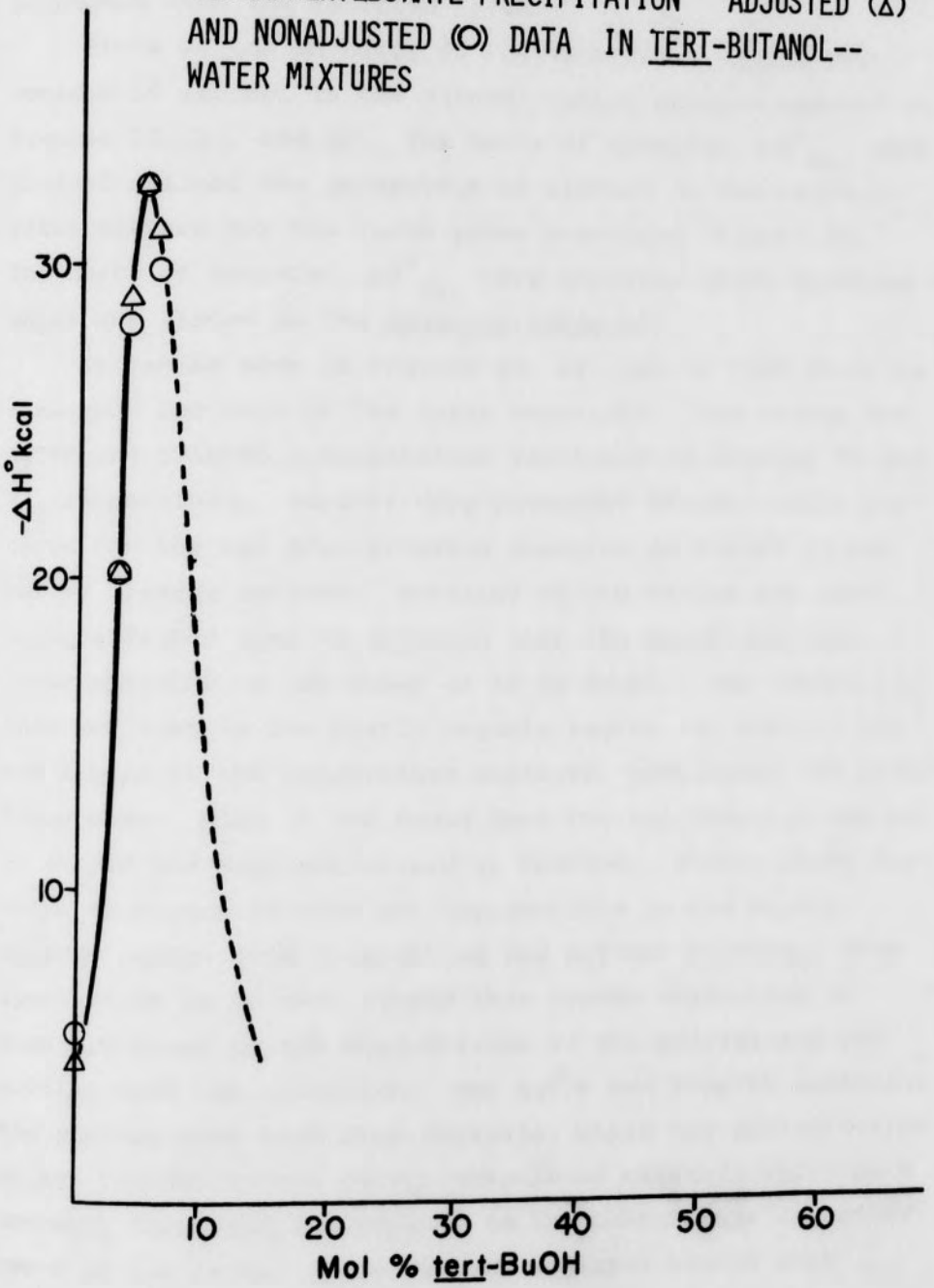

water. The experimental enthalpy value obtained was in good agreement with the reported value.

Plots of the enthalpy of reaction, ΔH^{o}, *versus* percentage of alcohol in the alcohol--water mixture appears in Figures 20, 21, and 22. The heats of transfer, $\Delta H^{o}_{tr,}$ were plotted against the percentage of alcohol in the alcohol--water mixture for the three probe reactions (Figure 23). The heats of transfer, $\Delta H^{o}_{tr,}$ were obtained using Equation 4 which was listed in the *Research Proposal*.

It can be seen in Figures 20, 21, and 22 that there is a maximum for each of the three reactions. The curves for AgTPB and TPAsTPB precipitation reactions in Figures 21 and 22, respectively, exhibit very prominent maxima, while the curve for the AgI precipitation reaction in Figure 20 was not so clearly defined. Portions of the curves are drawn using a dashed line to indicate that the exact position of these sections is not known or is in doubt. One reason for this was that in the highly organic region the mixture was not liquid at the temperature employed, precluding the titrations here. Also it was found that the AgI reaction was not as simple and straightforward as thought. Points along the curve in Figure 20 were not reproducible in the highly aqueous region (~5% alcohol) of the solvent mixture. Some speculation as to what caused this random scattering is possible based on the observations of the precipitate resulting from the titration. For AgTPB and TPAsTPB reactions the precipitates were fine crystals, while the precipitation of AgI yielded rather curdy, coagulated crystals which were unevenly dispersed and adhered to the thermistors and other parts of the cell. These factors may have caused poor

FIGURE 20. ENTHALPY OF REACTION FOR SILVER IODIDE PRECIPITATION (ADJUSTED DATA) IN TERT-BUTANOL--WATER MIXTURES

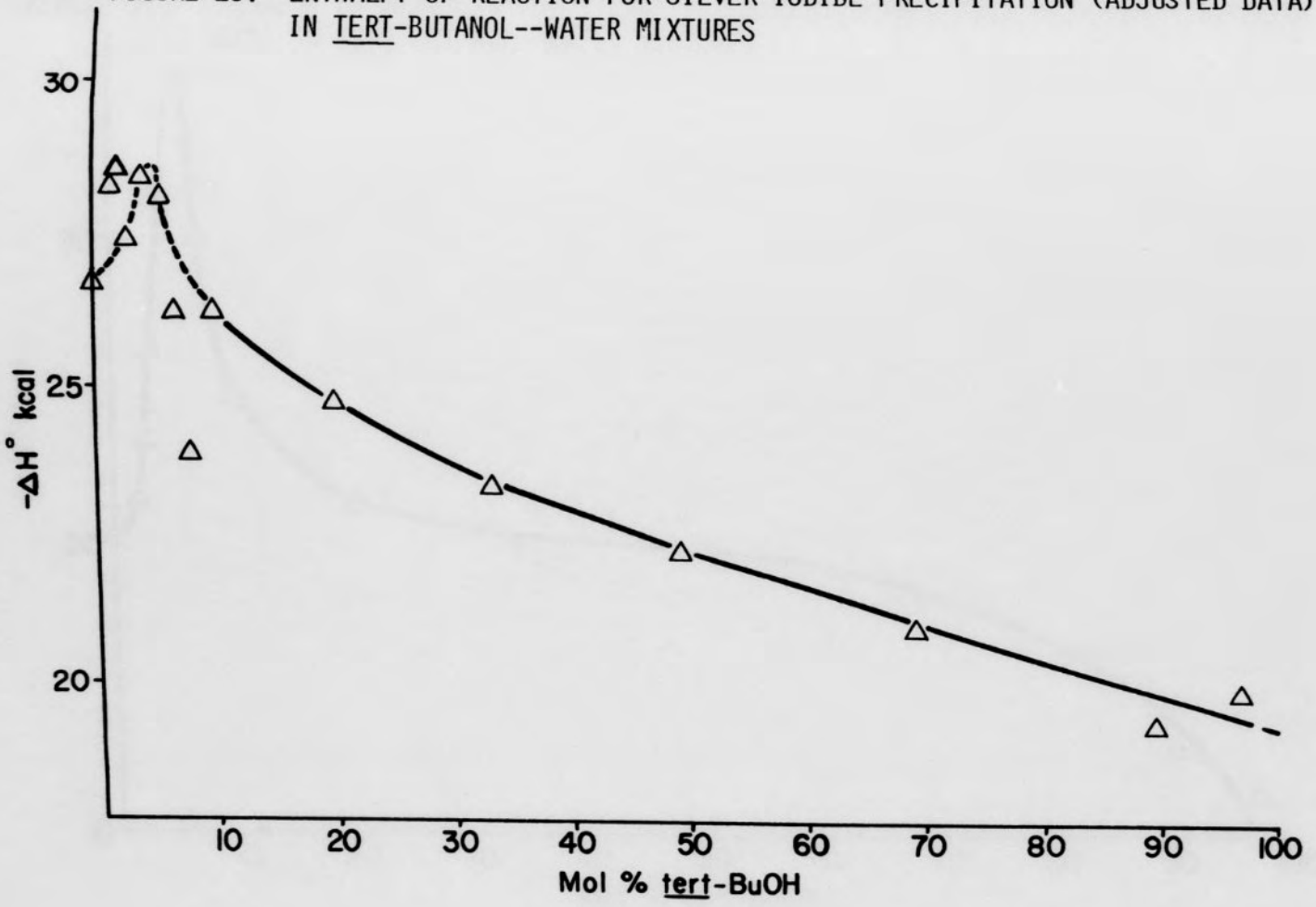

FIGURE 21. ENTHALPY OF REACTION FOR SILVER TETRAPHENYLBORATE PRECIPITATION (ADJUSTED DATA) IN TERT-BUTANOL--WATER MIXTURES

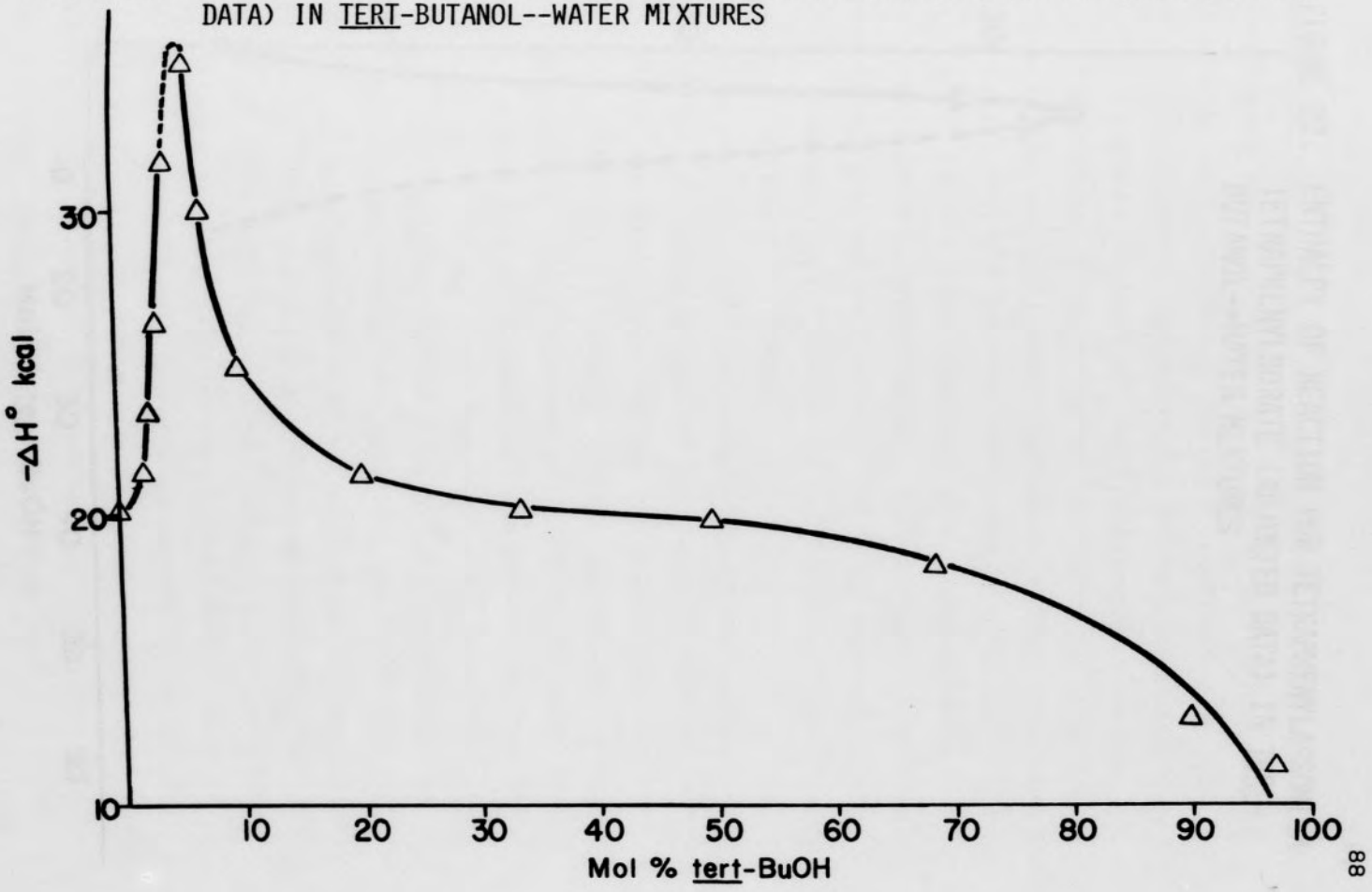

FIGURE 22. ENTHALPY OF REACTION FOR TETRAPHENYLARSONIUM TETRAPHENYLBORATE (ADJUSTED DATA) IN TERT-BUTANOL--WATER MIXTURES

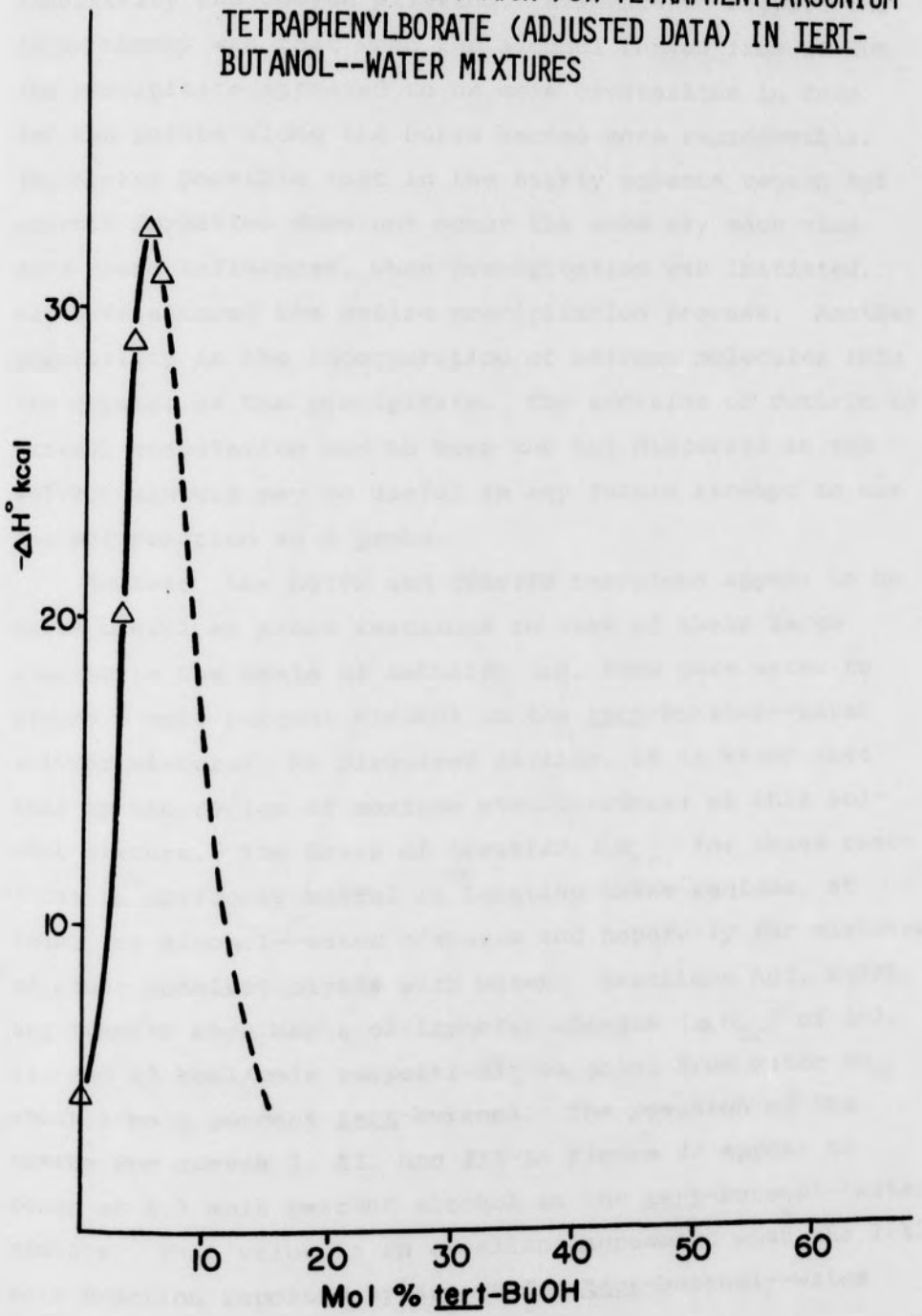

sensitivity and uneven stirring. Evidence to support the above theory was that when the alcohol ranged from 10-80%, the precipitate appeared to be more crystalline in form and the points along the curve became more reproducible. It is also possible that in the highly aqueous region AgI crystal formation does not occur the same way each time. Some micro influences, when precipitation was initiated, may have altered the entire precipitation process. Another possibility is the incorporation of solvent molecules into the crystal of the precipitate. The addition of dextrin to prevent coagulation and to keep the AgI dispersed in the solvent mixture may be useful in any future attempt to use the AgI reaction as a probe.

However, the AgTPB and TPAsTPB reactions appear to be quite useful as probe reactions in view of their large changes in the heats of enthalpy, ΔH, from pure water to around 5 mole percent alcohol in the tert-butanol--water solvent mixture. As discussed earlier, it is known that this is the region of maximum structuredness of this solvent mixture. The heats of transfer, $\Delta H_{tr,}$ for these reactions is obviously useful in locating these regions, at least for alcohol--water mixtures and hopefully for mixtures of other nonelectrolytes with water. Reactions AgI, AgTPB, and TPAsTPB show heats of transfer changes (ΔH_{tr}) of 5-7, 15, and 27 kcal/mole respectively on going from water to about 5 mole percent tert-butanol. The position of the maxima for curves I, II, and III in Figure 23 appear to occur at 5.3 mole percent alcohol in the tert-butanol--water mixture. This value is in excellent agreement with the 1:17 mole fraction reported by Arnett for tert-butanol--water

FIGURE 23. HEAT OF TRANSFER FROM WATER TO TERT-BUTANOL--WATER MIXTURES (I=SILVER IODIDE; II=SILVER TETRAPHENYLBORATE; III=TETRAPHENYLARSONIUM TETRAPHENYLBORATE)

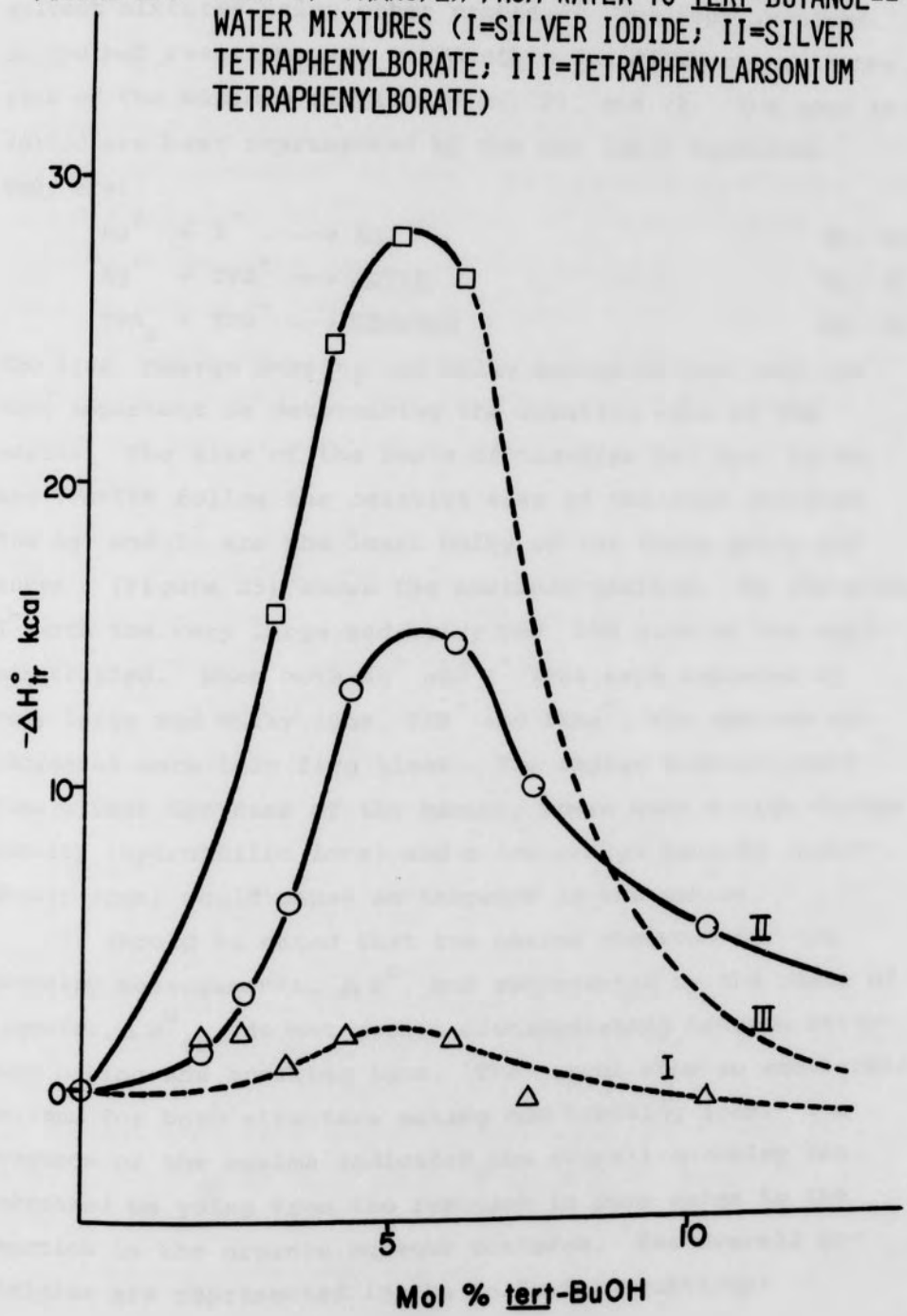

solvent mixtures using other probes.[35] The ions involved in the net reactions are responsible for differences in the size of the maximum in Figures 20, 21, and 22. The ions involved are best represented by the net ionic equations. They are:

$$Ag^+ + I^- \longrightarrow \underline{AgI} \qquad \text{Eq. 50}$$

$$Ag^+ + TPB^- \longrightarrow \underline{AgTPB} \qquad \text{Eq. 51}$$

$$TPA_s + TPB^- \longrightarrow \underline{TPAsTPB} \qquad \text{Eq. 52}$$

The size, charge density and bulky nature of the ions are very important in determining the relative size of the maxima. The size of the heats of transfer for AgI, AgTPB, and TPAsTPB follow the relative size of the ions involved. The Ag^+ and I^- are the least bulky of the three pairs and curve I (Figure 23) shows the smallest maximum. By replacing I^- with the very large and bulky TPB^- the size of the maximum tripled. When both Ag^+ and I^- ions were replaced by very large and bulky ions, TPB^- and $TPAs^-$, the maximum was increased more than five times. The charge density could also affect the size of the maxima, where both a high charge density (hydrophilic ions) and a low charge density (hydrophobic ions) would cause an increase in the maxima.

It should be noted that the maxima observed for the enthalpy measurements, ΔH^o, and represented by the heats of transfer, ΔH^o_{tr}, do not permit distinguishing between structure making and breaking ions. The curves show an exothermic maximum for both structure making and breaking ions. The presence of the maxima indicated the overall enthalpy has increased on going from the reaction in pure water to the reaction in the organic aqueous mixtures. The overall enthalpies are represented in the following equations:

$$\Delta H^{o}_{H_2O} = \Delta H^{o}_{c,a,f,cryst\ (H_2O)} + \Delta H^{o}_{st(H_2O)} \qquad \text{Eq. 53}$$

$$\Delta H^{o}_{mix} = \Delta H^{o}_{c,a,f,cryst\ (mix)} + \Delta H^{o}_{st(mix)} \qquad \text{Eq. 54}$$

where the terms c,a,f,cryst , and st have the same meaning as before. Assuming the ions involved were structure breakers, their removal by precipitation would cause an increase in structure, an exothermic process. Since the ions would have more structure to break in the highly aqueous tert-butanol--water mixture than in pure water, it follows that as structure breaking ions are removed, more reformation of the structure results where more structure had been broken. Therefore,

$$-\Delta H^{o}_{st(mix)} > -\Delta H^{o}_{st(H_2O)} \qquad \text{Eq. 55}$$

It follows from the relations of equations 53, 54, and 55, assuming that $\Delta H^{o}_{c,a,f,cryst}$ is essentially unchanged on going from pure water to the mixtures, that

$$\Delta H^{o}_{(mix)} > \Delta H^{o}_{H_2O} \qquad \text{Eq. 56}$$

Hence the overall enthalpies measured in the highly aqueous tert-butanol--water region are more exothermic because the $\Delta H^{o}_{st(mix)}$ is more exothermic than the $\Delta H^{o}_{st(H_2O)}$ contribution. If on the other hand the ions were structure makers, the removal by precipitation would result in an overall structure collapse, an endothermic process. Since the ions are not able to make as much structure in the highly aqueous region of the tert-butanol--water mixture as in pure water, it follows that as structure making ions are removed more structure collapse will occur where more structure had been formed. Therefore,

$$+\Delta H^{o}_{st(mix)} < +\Delta H^{o}_{st(H_2O)} \qquad \text{Eq. 57}$$

It follows using equations 53, 54, and 57 that:

$$\Delta H^{o}_{(mix)} > \Delta H^{o}_{(H_2O)} \qquad \text{Eq. 58}$$

when the other enthalpy terms involved are approximately unchanged. Hence overall enthalpies measured in the highly aqueous tert-butanol--water region are more exothermic because the $\Delta H^{o}_{st(mix)}$ is less endothermic than the $\Delta H^{o}_{st(H_2O)}$ contribution.

Ag^{+} and I^{-} have both been previously characterized as structure breakers.[81] Iodide has been shown to be the most extensive structure breaker of the halogens because of its size and small charge concentration. The small size and larger charge density of the Ag^{+} makes it a weaker structure breaker than I^{-}. When comparing I^{-} and TPB^{-} the size and the seemingly hydrophobic characteristic of the phenyl groups would at first glance make it a structure maker. The size and charge density comparison would indicate it to be a structure breaker because the smaller the charge density and the larger the size the greater is its structure breaking ability. At the present time, as mentioned before, the question as to whether ions containing phenyl groups such as $TPAs^{+}$ and TPB^{-} are structure makers or structure breakers has not been settled. It is fairly certain that the size of the TPB^{-} as compared to the I^{-} would make a more structure altering ion, whether structure making or breaking. The results do show a very large maximum for the ions containing phenyl groups, indicating that the seemingly opposing factors of size and charge density (structure breaking) and of the size hydrocarbon portion of the molecule (nominally structure making) do not cancel each other out. Our results may shed

some light on this problem using the enthalpy and solubility constant, K_{sp}, values to calculate the entropy of reaction.

$$\Delta F^{\circ} = RT\ln K \qquad \text{Eq. 59}$$

$$\Delta F^{\circ} = \Delta H^{\circ} - T\Delta S^{\circ} \qquad \text{Eq. 60}$$

where ΔG° is the free energy of reaction. The entropies, ΔS°, are listed for precipitation of AgI and AgTPB in Table 12.[78,82] The ΔS° for TPAsTPB could not be obtained as to our knowledge no equilibrium constant is available.

TABLE 12

Thermodynamic Values for Precipitation Reactions at 25°C

Reactions	ΔH° (kcal/mole)	ΔF° (kcal/mole)	ΔS° (kcal/mole)	K_{sp}
$Ag^{+} + I^{-} \rightarrow AgI$	-26.7	-21.6	-17.2	1.5×10^{-16}
$Ag^{+}\ TPB^{-} \rightarrow AgTPB$	-20.2	-23.5	+11.0	6.3×10^{-18}

The negative entropy, ΔS°, for the AgI precipitation reaction indicates an overall increase in order for the precipitation reaction, consistent with the I^{-} as a structure breaker. The positive entropy, ΔS°, for the AgTPB precipitate reaction seems to imply that TPB^{-} is a structure maker. The Ag^{+}, which was common in both reactions, was previously mentioned as being a slight structure breaker. This would then suggest that the $\sim$ +28 units entropy difference for the two reactions is due to the TPB^{-}, strongly implying a structure making character. The $TPAs^{+}$ might also be suggested to be a structure maker in view of the similarity in the number of phenyl groups and size but this idea does not take into consideration the difference in charge density of the two ions. The presence of the phenyl groups suggest that $TPAs^{+}$ is a structure making species because of the hydrocarbon (hydrophobic)

character. Obviously, more data is needed to resolve this conflict.

Originally, slightly soluble salts of divalent mercury and lead were considered as possible probe reactions. However, when Hg^{2+} and $Pb^{2}+$ were precipitated with NaI, the enthalpograms obtained revealed two distinct nonlinear sections in the titration curve. These complex enthalpograms proved difficult to interpret and the enthalpy values calculated were in poor agreement with the reported values. Thus these reactions were discarded as useful probe reactions. The use of Hg_2I_2 as a reaction probe was also unsuccessful. Some undetermined characteristics of the reaction caused a large nonlinear portion in the titration curve.

VII. SUMMARY

This investigation has provided data that shows that the heat of transfer of slightly soluble salts *via* precipitation titrations is an excellent probe for the study of water structure changes. The $AgClO_4$-NaTPB and TPAsCl-NaTPB reactions should prove very useful in studying other organic--aqueous solvent systems for which the structural interactions are unknown. The overall size and hydrocarbon nature of the ions have been shown to be important in predicting the size of the ΔH^{o}_{tr} maxima expected. The data also implies the possibility that ions containing phenyl groups are structure makers, although more data must be collected before a definite statement can be made. If this is correct for ions of this type, the method may prove very useful in distinguishing whether ions are structure makers or breakers. The accumulation of such behavioral data and other data will have an influence in the study of solvent effects of organic--aqueous systems and in the development of a liquid water model that will explain the unique character of water.

BIBLIOGRAPHY

1. F. Franks in "Water a Comprehensive Treatise," Vol. 1 The Physics and Physical Chemistry of Water, F. Franks, Ed. Plenum Press, New York, N. Y., 1972, Chapter 1.

2. H. H. V. Vernon, Phil. Mag. 31, 387 (1891).

3. W. K. Röntgen, Ann. Phys. 45, 91 (1892).

4. W. Sutherland, Phil. Mag. 50, 460 (1900).

5. J. D. Bernal and R. H. Fowler, J. Chem. Phys. 1, 515 (1933).

6. H. S. Frank and M. Evans, ibid., 13, 507 (1945).

7. H. S. Frank, Science, 169, 635 (1970).

8. M. D. Danford and H. A. Levy, J. Amer. Chem. Soc. 84, 3965 (1962).

9. L. Pauling, "The Nature of the Chemical Bond," 3rd ed. Cornell University Press, Ithaca, N. Y., 1960, p 469.

10. J. A. Pople, Proc. Roy. Soc. London Ser. A Math. Phys. Sci. 205, 163 (1951); Chem. Abstr. 45, 5986d (1951).

11. H. S. Frank and W. Y. Wen, Dis. Faraday Soc. 24, 133 (1957).

12. G. H. Haggis, B. J. Hasted, and T. J. Buchanan, J. Chem. Phys. 20, 1452 (1952).

13. G. E. Walrafen, ibid., 47, 114 (1967).

14. A. S. N. Murthy and C. N. R. Rao, J. Mol. Struct. 6, 253 (1970); Chem. Abstr. 73, 113043s (1970).

15. C. N. R. Rao in "Water a Comprehensive Treatise," Vol. 1 The Physics and Physical Chemistry of Water, F. Franks, Ed., Plenum Press, New York, N. Y., 1972, Chapter 3.

16. A. S. N. Murthy and C. N. R. Rao, Chem. Phys. Letters, 2, 123 (1968); Chem. Abstr. 69, 54358r (1968).

17. A. Goel, A. S. N. Murthy, and C. N. R. Rao, Indian J. Chem. 9, 56 (1971).

18. J. R. Hoyland and L. B. Kier, Theor. Chim Acta, 15, 1 (1969); Chem. Abstr. 71, 11658r (1969).

19. J. DelBene and J. A. Pople, Chem. Phys. Letters, 4, 426 (1969); Chem. Abstr. 72, 47599d (1970).

20. G. E. Walrafen, J. Chem. Phys. 48, 244 (1968).

21. G. E. Walrafen in "Hydrogen-Bonded Solvent System," A. K. Covington and P. Jones, Eds., Taylor and Francis, London, 1968, pp 9-29.

22. G. E. Walrafen, J. Chem. Phys. 50, 560 (1969).

23. G. E. Walrafen, ibid., 50, 567 (1969).

24. G. E. Walrafen, ibid., 52, 4176 (1970).

25. G. E. Walrafen, ibid., 44, 1546 (1966).

26. J. E. Bertie, H. J. Labbe, and E. Whalley, ibid., 50, 4501 (1969).

27. G. E. Walrafen, ibid., 40, 3249 (1964).

28. K. E. Larsson and U. Dahlborg, Reactor Sci. Tech., J. Nucl. Energy, 16, 81 (1962); Chem. Abstr. 63, 17172a (1965).

29. G. E. Walrafen in "Water a Comprehensive Treatise," Vol. 1 The Physics and Physical Chemistry of Water, F. Franks, Ed., Plenum Press, New York, N. Y., 1972, Chapter 5.

30. J. Morgan and B. E. Warren, J. Chem. Phys. 6, 666 (1968).

31. A. H. Narten and H. A. Levy in "Water a Comprehensive Treatise," Vol. 1 The Physics and Physical Chemistry of Water, F. Franks, Ed., Plenum Press, New York, N. Y., 1972, Chapter 8.

32. S. Shibata and L. S. Bartell, J. Chem. Phys. 42, 1147 (1965).

33. S. LaPlaca and B. Post, Acta Cryst. 13, 503 (1960).

34. F. Franks and D. J. G. Ives, Quart. Rev. 20, 1 (1966).

35. E. M. Arnett in "Physico-Chemical Processes in Mixed Aqueous Solvents," F. Franks, Ed., American Elsevier Publishing Company, Inc., New York, N. Y., 1969, pp 105-128.

36. W. H. Zachariasen, J. Chem. Phys. 3, 158 (1935).

37. G. G. Harvey, ibid. 6, 111 (1938).

38. G. G. Harvey, ibid. 7, 878 (1939).

39. F. F. Harris, E. W. Haycock, and B. J. Alder, ibid., 21, 19 (1943).

40. G. A. Miller, J. Chem. Eng. Data, 9, 418 (1964).

41. J. J. McKetta, J. Phys. Chem. 66, 1444 (1962).

42. B. Lemanceau, C. Lussan, and N. Souty, J. Chim. Phys. 59, 148 (1962); Chem. Abstr. 56, 13693e (1962).

43. C. Reid and T. M. Conner in "Hydrogen Bonding," Hadzi and H. W. Thompson, Eds., Pergamon Press, London, 1959, Chapter 3.

44. S. Winstein and A. H. Fainberg, J. Amer. Chem. Soc. 79, 5937 (1957).

45. C. J. Burton, J. Acoust. Soc. Amer. 20, 186 (1948).

46. I. Lee and J. B. Hyne, Can. J. Chem. 46, 2333 (1968).

47. F. Franks in "Physico-Chemical Processes in Mixed Aqueous Solvents," F. Franks, Ed., American Elsevier Publishing Co., Inc., New York, N. Y., 1969, pp 50-70.

48. I. I. Bezman and F. H. Verhock, J. Amer. Chem. Soc. 67, 1330 (1945).

49. E. M. Arnett and D. Hufford, ibid. 88, 3140 (1966).

50. G. A. Jeffrey, "Progress in Inorganic Chemistry," Vol. VIII, F. A. Cotton, Ed., Interscience Publishers, Inc., New York, N. Y., 1967, pp 43-108.

51. J. E. Desnoyers, M. Arel, and C. Jolicoeur, J. Phys. Chem. 73, 3346 (1969).

52. G. Kalfoglou and L. D. Brown, ibid. 73, 2728 (1969).

53. F. J. Millero, Chem. Rev. 71, 147 (1971).

54. R. K. Moharty and J. C. Ahluwalia, J. Chem. Thermodynamics, 4, 53 (1972).

55. C. Jolicoeur, P. R. Philip, G. Perron, P. A. Ledue, and J. E. Desnoyers, Can. J. Chem. 50, 3167 (1972).

56. J. R. Jezorek, University of N. C. at Greensboro, personal communication, 1973.

57. S. T. Zenchelsky, Anal. Chem. 32, 289R (1960).

58. J. M. Bell and C. F. Cowell, J. Am. Chem. Soc. 35, 49 (1913).

59. P. Dutoit and E. Grobet, J. Chim. Phys. 19, 324 (1922); Chem. Abstr. 16, 3041 (1922).

60. H. W. Linde, L. B. Rogers, and D. N. Hume, Anal. Chem. 25, 404 (1953).

61. J. Jordan and T. G. Alleman, ibid. 29, 9 (1957).

62. B. C. Tyson, Jr., W. H. McCurdy, Jr., and C. E. Bricker, ibid. 33, 1640 (1961).

63. R. M. Izatt, D. Eatough, R. L. Snow, and J. J. Christensen, J. Phys. Chem. 72, 1208 (1968).

64. J. Jordon, Anal. Chem. 40, A5 (1963).

65. P. T. Priestly, Analyst, 88, 194 (1963).

66. E. B. Smith, C. S. Barnes, and P. W. Carr, Anal. Chem. 44, 1663 (1972).

67. M. Nakanishi and S. Fujieda, ibid. 44, 575 (1972).

68. J. J. Christensen, H. D. Johnston, and R. M. Izatt, Rev. Sci. Instrum. 39, 1356 (1968).

69. J. C. Wasilewski, P. T-S. Pei, and J. Jordan, Anal. Chem. 36, 2133 (1964).

70. L. S. Bark and S. M. Bark, "Thermometric Titrimetry," Pergamon Press, New York, N. Y., 1969, p 6.

71. J. Jordan in "Treatise on Analytical Chemistry," Part 1, Theory and Practice, Vol. 8, I. M. Kolthoff, P. J. Elving, and E. D. Sandell, Eds., Interscience Publishers, John Wiley and Sons, New York, N. Y., 1968, Section D5.

72. J. J. Christensen, R. M. Izatt, and L. D. Hansen, Rev. Sci. Instrum. 36, 779 (1965).

73. P. W. Carr and J. Jordan, Anal. Chem. 44, 1278 (1972).

74. P. W. Carr, CRC Critical Reviews in Analytical Chemistry, 10, 491 (1972).

75. J. J. Christensen and R. M. Izatt in "Physical Methods in Advanced Inorganic Chemistry," H. A. O. Hill and P. Day, Eds., Interscience Publishers, John Wiley and Sons, Inc., New York, N. Y., 1968, Chapter 11.

76. T. DeVries and H. Soffer, J. Phys. Chem. 55, 406 (1951).

77. W. T. Bolleter and R. J. Baczuk, Anal. Chem. 39, 93 (1967).

78. R. C. Weast, Ed. "Handbook of Chemistry and Physics," 51st ed., The Chemical Rubber Company, Cleveland, Ohio, 1970-71.

79. B. D. Faithful and S. C. Wallwork, Acta Cryst. B28, 2301 (1972).

80. P. G. Stecher, M. Windholz, and D. S. Leahy, Eds. "The Merck Index," Merck and Co., Inc., Rahway, N. J. (1968).

81. J. R. Jezorek, Ph.D. Thesis, University of Delaware, Newark, Del., 1969.

82. F. D. Rossini, D. D. Wagman, W. H. Evans, S. Levine, and I. Jaffe, "Selected Values of Chemical Thermodynamic Properties," Government Printing Office, Washington, D. C., 1954.

83. I. M. Kolthoff and M. K. Chantooni, Jr., Anal. Chem. 44, 194 (1971).

APPENDIX

Computer Program for Enthalpy Calculations

```
1.        DIMENSION HNUM(10),HDEN(10),HNUB(10),HDEB(10)
         *,SLOPE(10),ENTHAL(10),DEV(12),AVENTH(12)
      C  THE NUMBER OF GROUPS OF TITRATION CURVES ARE READ IN
2.        READ, K
3.        DO 70 L = 1,K
      C  THE NUMBER OF TITRATION CURVES ARE READ IN
4.        READ, M
5.        SUMHT = O
6.        DO 40 J = 1,M
      C  THE NUMBER OF HEATING CURVES IS READ IN
7.        READ, N
      C    THE NUMERATORS AND DENOMINATORS OF HEATING CURVE
         *SLOPES
      C    AND BASE LINES ARE READ IN
8.        READ, (HNUM(I), HDEN(I), HNUB(I), HDEB(I), I=1,N)
      C    THE TITRATION CURVE SLOPE AND BASE LINE NUMERATORS
         *AND DENOMINATORS
      C    ARE READ IN
9.        READ, TNUM, TDEN, TNUB, TDEB
      C  THE HEATER AND STD. RESISTOR VOLTAGES, TITRANT CONCS.
         *AND FLOW RATES
      C  ARE READ IN
10.       READ, HTVOLT, SRVOLT, CONC, FLOW
      C  EACH HEATING CURVE SLOPE IS CALCULATED
11.         DO 10 I=1,N
12.       10 SLOPE(I) = HNUM(I)/HDEN(I) + HNUB(I)/HDEB(I)
      C  THE SUM OF THE HEATING CURVES IS CALCULATED
```

```
13          HEAT = 0
14.         DO 20 I = 1,N
15.       20 HEAT = HEAT + SLOPE(I)
      C    THE HEATING CURVE AVERAGE IS CALCULATED
16.         HEATAV = HEAT/FLOAT(N)
      C    THE TITRATION CURVE SLOPE IS CALCULATED
17.         TITRA = TNUM/TDEN + TNUB/TDEB
      C    THE ENTHALPY FOR EACH HEATING CURVE IS CALCULATED
18.         DO 30 I = 1,N
19.       30 ENTHAL(I) = HTVOLT*SRVOL*TITRA/(4.185*CONC*FLOW*
           *SLOPE*(I))
      C  THE AVERAGE ENTHALPY FOR EACH TITRATION IS CALCULATED
20.         AVENTH(J) = HTVOLT*SRVOLT*TITRA/(4.185*CONC*FLOW
           *HEATAV)
      C  THE AVERAGE ENTHALPY FOR ALL TITRATIONS IS CALCULATED
21.         SUMHT = SUMHT + AVENTH(J)
22.         DELTAH = SUMHT/FLOAT(M)
      C  THE INPUT DATA AND RESULTS ARE PRINTED OUT
23.         PRINT  'HTVOLT = ', HTVOLT, 'SRVOLT = ', SRVOLT,
           *'CONC = ', CONC, 'FLOW RATE = ', FLOW
24.         PRINT, 'HEATING SLOPE VALUES = ', (SLOPE(I),
           *I = 1,N)
25.         PRINT, 'HEATING SLOPE AVG = ', HEATAV
26.         PRINT, 'TITRATION CURVE SLOPE = ', TITRA
27.         PRINT  ' ENTHALPIES = ', (ENTHAL(I), I = 1,N)
28.         PRINT, 'ENTHALPY AVG = ', AVENTH(J)
29.       40 CONTINUE
30.         DO 50 J = 1,M
31.       50 DEV(J) = DELTAH - AVENTH(J)
32.         SUMDEV = O
```

```
33.          DO 60 J = 1,M
34.       60 SUMDEV = SUMDEV + ABS(DEV(J))
35.          AVGDEV = SUMDEV/FLOAT(M)
36.          RELDEV = 100.0*AVGDEV/DELTAH
37.          PRINT, ' THE DEVIATIONS FROM THE MEAN = ', (DEV(J)
             *, J = 1,M)
38.          PRINT, ' THE OVERALL ENTHALPY AVERAGE = ', DELTAH,
             *' THE AVERAGE DEVIATION FROM THE MEAN = ', AVGDEV
39.          PRINT, ' THE RELATIVE AVERAGE DEVIATION FROM THE
             *MEAN IN % = ', RELDEV
40.          WRITE(3,124)
41.       124 FORMAT('1')
42.        70 CONTINUE
43.           STOP
44.           END

           $DATA
HTVOLT =       0.1397000E 01 SRVOLT =      0.6849998E-01 CONC =
              *0.8660299E-01 FLOW RATE =  0.1056000E-01

HEATING SLOPE VALUES =     0.8701443E 00     0.8476143E 00
                          *0.8790908E 00

HEATING SLOPE AVG =       0.8656161E 00

TITRATION CURVE SLOPE =       0.6908190E 00

 ENTHALPIES =     0.1985031E 02     0.2037794E 02
                 *0.1964828E 02

ENTHALPY AVG =       0.1995415E 02

HTVOLT =       0.1406000E 01 SRVOLT =       0.6889999E-01 CONC =
              *0.8660299E-01 FLOW RATE =       0.1056000E-01

HEATING SLOPE VALUES =       0.8883439E 00       0.8835396E 00
                            *0.8921287E 00

HEATING SLOPE AVG =       0.8880036E 00
```

```
TITRATION CURVE SLOPE =      0.6955940E 00

 ENTHALPIES =      0.1981921E 02      0.1992699E 02
                  *0.1973514E 02

ENTHALPY AVG =      0.1982681E 02

HTVOLT =      0.1406000E 01 SRVOLT =      0.6889999E-01 CONC =
              *0.8660299E-01 FLOW RATE =      0.1056000E-01

HEATING SLOPE VALUES =      0.8858259E 00      0.8860537E 00

HEATING SLOPE AVG =      0.8859396E 00

TITRATION CURVE SLOPE =      0.7135664E 00

 ENTHALPIES =      0.2038908E 02      0.2038385E 02

ENTHALPY AVG. =      0.2038647E 02

THE DEVIATIONS FROM THE MEAN =      0.1016541E 00
                                   *0.2289886E 00
                                   *-0.3306732E 00

THE OVERALL ENTHALPY AVERAGE =      0.2005580E 02  THE AVERAGE
                                   *DEVIATION FROM THE MEAN =
                                   *0.2204386E 00

THE RELATIVE AVERAGE DEVIATION FROM THE MEAN IN % =
                                   *0.1099126E 01

HTVOLT =      0.1772000E 01 SRVOLT =      0.8700001E-01 CONC =
              *0.8290201E-01 FLOW RATE =      0.1056000E-01

HEATING SLOPE VALUES =      0.1346580E 01      0.1377566E 01
                           *0.1387300E 01

HEATING SLOPE AVG =      0.1370481E 01

TITRATION CURVE SLOPE =      0.1053364E 01

 ENTHALPIES =      0.3291583E 02      0.3217545E 02
                  *0.3194968E 02

ENTHALPY AVG =      0.3234177E 02

HTVOLT =      0.1773000E 01 SRVOLT =      0.8710003E-01 CONC =
              *0.8290201E-01 FLOW RATE =      0.1056000E-01
```

```
HEATING SLOPE VALUES =      0.1389778E 01     0.1391778E 01
                           *0.1375214E 01

HEATING SLOPE AVG =      0.1385590E 01

TITRATION CURVE SLOPE =      0.1079318E 01

 ENTHALPIES =      0.3273454E 02     0.3268753E 02
                  *0.3308124E 02

ENTHALPY AVG =      0.3283351E 02

HTVOLT =      0.1772000E 01 SRVOLT =      0.8700001E-01 CONC =
             *0.8290201E-01 FLOW RATE =      0.1056000E-01

HEATING SLOPE VALUES =      0.1377977E 01     0.1371897E 01

HEATING SLOPE AVG =      0.1374937E 01

TITRATION CURVE SLOPE =      0.1045566E 01

 ENTHALPIES =      0.3192770E 02     0.3206921E 02

ENTHALPY AVG =      0.3199831E 02

THE DEVIATIONS FROM THE MEAN =      0.4942322E-01
                                   *-0.4423218E 00
                                   *0.3928833E 00

THE OVERALL ENTHALPY AVERAGE =      0.3239119E 02 THE AVERAGE
                                   *DEVIATION FROM THE MEAN =
                                   *0.2948761E 00

THE RELATIVE AVERAGE DEVIATION FROM THE MEAN IN % =
                                   *0.9103590E 00

HTVOLT =      0.1610000E 01 SRVOLT =      0.7900000E-01 CONC =
             *0.9174597E-01 FLOW RATE =      0.1056000E-01

HEATING SLOPE VALUES =      0.1153350E 01     0.1141595E 01
                           *0.1132825E 01

HEATING SLOPE AVG =      0.1142590E 01

TITRATION CURVE SLOPE =      0.1118374E 01

 ENTHALPIES =      0.3041812E 02     0.3073132E 02
                  *0.3096927E 02

ENTHALPY AVG =      0.3070459E 02
```

```
HTVOLT =      0.1610000E 01 SRVOLT =      0.7900000E-01 CONC =
             *0.9174597E-01 FLOW RATE =      0.1056000E-01

HEATING SLOPE VALUES =      0.1181979E 01      0.1182478E 01
                           *0.1186486E 01

HEATING SLOPE AVG =      0.1183647E 01

TITRATION CURVE SLOPE =      0.1182371E 01

 ENTHALPIES =      0.3137981E 02      0.3136659E 02
                  *0.3126062E 02

ENTHALPY AVG =      0.3133560E 02

HTVOLT =      0.1610000E 01 SRVOLT =      0.7900000E-01 CONC =
             *0.9174597E-01 FLOW RATE =      0.1056000E-01

HEATING SLOPE VALUES =      0.1178711E 01      0.1191967E 01
                           *0.1203669E 01

HEATING SLOPE AVG =      0.1191448E 01

TITRATION CURVE SLOPE =      0.1177126E 01

 ENTHALPIES =      0.3132724E 02      0.3097884E 02
                  *0.3067767E 02

ENTHALPY AVG =      0.3099231E 02

THE DEVIATIONS FROM THE MEAN =      0.3062439E 00
                                   *-0.3247681E 00
                                   *0.1852417E-01

THE OVERALL ENTHALPY AVERAGE =      0.3101083E 02
                                   *THE AVERAGE DEVIATION FROM
                                   *THE MEAN =
                                   *0.2165120E 00

THE RELATIVE AVERAGE DEVIATION FROM THE MEAN IN % =
                                   *0.6981817E 00
```